McEachran Zac (Orcid ID: 0000-0002-7221-8047)
Karwan Diana (Orcid ID: 0000-0002-4529-0369)

**Effects of forest disturbance on water yield and peak flow in low-relief glaciated catchments assessed with Bayesian parameter estimation**

McEachran, Zachary P.[1*], Reese, Gordon C.[2]; Karwan, Diana L.[3]; Slesak, Robert A.[4]; Vogeler, Jody[5]

[1] NOAA National Weather Service North Central River Forecast Center, Chanhassen, MN 55317

[2] USDA Forest Service, Northern Research Station, Rhinelander, WI, USA 54501

[3] University of Minnesota, Department of Forest Resources, St. Paul, MN 55108

[4] USDA Forest Service, Pacific Northwest Research Station, Olympia, WA 98512

[5] Natural Resources Ecology Laboratory, Colorado State University, Fort Collins, CO 80526

* zachary.mceachran@noaa.gov

*Data Availability*

All data utilized are publicly available and are cited in the paper, including where these datasets may be obtained. The exception is the annual-scale forest disturbance maps used in the St. Louis Basin analysis, which are part of an in-preparation paper led by Dr. Vogeler and will be available upon its publication.

*Conflict of Interest*

None of the authors have a conflict of interest to disclose

## Abstract

Empirical assessment of how forest disturbance affects streamflow has been traditionally limited to small, experimental catchments. However, larger catchments where landscape management occurs have emergent drivers of streamflow at scale, and thus may exhibit novel responses to land cover disturbance. We used statistical models of water yield and annual maximum peak streamflow for multiple large (> 50 km$^2$) forested catchments in the low-relief glaciated region of central North America to investigate how forest disturbance and climatic variability affect water yield and peak flows in similar landscapes. We used linear models, linear mixed effects models, and probabilistic flood-frequency analysis with Bayesian parameter estimation in two case studies. These included: 1) a wildfire that burned ~30% of the 650 km$^2$ wilderness Upper Kawishiwi catchment, and 2) 11 catchments within the St. Louis River Basin ranging from 56 to 8,880 km$^2$ with a patchwork disturbance regime wherein ~0.25% to 1% of the catchment is harvested or converted to non-forest land use each year. We also assessed the most likely hydrological recovery year after forest disturbance, and the relative importance of stationary and nonstationary drivers of streamflow. We found forest disturbance correlated with declines in water yield for low-level disturbance regimes in some catchments, but that water yield increased in response to the large-scale wildfire. Positive and negative associations of forest disturbance with peak flows were observed. Hydrologic recovery time ranged from 5 to 13 years for water yield and peak flows following disturbance. Despite these effects of forest disturbance on streamflow, effects of climatic variability and stationary catchment size factors were more prominent streamflow drivers. Basins larger than ~50 km$^2$ in low-relief glaciated regions can be impacted by forest cover change even on < 30% of basin area, but climatic variability and catchment spatial scale has a larger effect than forest disturbance.

## 1. Introduction

Some landscapes are managed as forest in part to maintain high-quality water supply for societal and ecosystem benefits (Andréassian, 2004). Forest disturbance, including anthropogenic and natural processes, can affect a catchment's water balance through decreases in evapotranspiration associated with loss of tree cover or tree mortality associated with the disturbance event (McEachran et al., 2020; Stednick, 1996). What effect forest cover change has on streamflow has been a key question widely investigated using empirical statistical analyses of catchment-scale data, often using a Before-After-Control-Impact (BACI) and paired watershed design focusing on experimental forest harvesting regimes (Neary, 2016). Key metrics of hydrologic change common in the literature include annual water yield and peak flows (Buttle, 2011), often defined as the annual maximum peak streamflow (Green & Alila, 2012; McEachran et al., 2021). Forest harvesting is the disturbance most often investigated, because of the experimental control in how the forest disturbance is implemented, in addition to relevance for forest and watershed management. In relatively small catchments, for each additional one percent that a catchment is harvested, annual water yield increases 0.5-7 mm/year (Bosch & Hewlett, 1982; Brown et al., 2005; Sahin & Hall, 1996; Stednick, 1996; Zhang et al., 2017). When forest land cover is converted to non-forest cover (or to another forest species composition), it takes several years (5-20+ years) to reach a new equilibrium water balance, while forest that is allowed to regenerate following disturbance utilizes water differently as it regrows through its life cycle (Brown et al., 2005). Often, 10-50% of a catchment has to be disturbed for discernible responses in water yield, but effects for much lower disturbance percentages have been found in some cases (Jones & Grant, 1996; Stednick, 1996). At all spatial scales, peak flow responses to forest harvesting are much more diverse and variable compared to effects on annual water yield including peak flows increasing, decreasing, or showing no effect (Alila et al., 2009; Buttle, 2011; Green & Alila, 2012; Guillemette et al., 2005; Jones & Grant, 1996; Thomas & Megahan, 1998). Some divergent results stem from methodological disagreement about the most appropriate framework within which to analyze peak flows (Bathurst et al., 2020; Alila et al., 2009; Jones & Grant, 1996; Thomas &

Megahan, 1998). Several review papers have described past empirical studies (e.g. Stednick 1996, Brown et al., 2005, Zhang et al 2017), but a full review is beyond the scope of our paper.

North American forest hydrology literature has mostly focused on the effect of forest harvesting in relatively steep, mountainous catchments (e.g., the Pacific Mountain System or Appalachian regions) (Goeking & Tarboton, 2020; Green & Alila, 2012; Hewlett & Hibbert, 1961; Jones & Grant, 1996; McEachran et al., 2020; Safeeq et al., 2020). Studies in central North America and Scandinavia have found forest harvesting to generally increase annual water yield, peak flows, and quickflow (Buttle et al., 2018; Buttle et al., 2019; Ide et al., 2013; McEachran et al., 2021; Sebestyen et al., 2011), but some variability has been found. For example, seasonal summer runoff can decrease in response to forest harvesting after a year of recovery, even while spring runoff remains elevated (Ide et al., 2013). Recovery to pre-treatment conditions for metrics of water yield and peak flows has been found to be between 10 and 20 years after harvest (Sebestyen et al., 2011), but some studies have not found a length of hydrologic recovery, with effects still detectable 15+ years after harvesting treatment (Buttle et al., 2018; Ide et al., 2013; McEachran et al., 2021). These results have supported management paradigms in the Great Lakes region of the north central USA to consider any forest that is less than or equal to 15 years old "young forest" that is potentially affecting water yield and peak flows, and any older forest as "hydrologically recovered" and effectively behaving as mature forest with respect to water balance components (Verry, 2004; Sebestyen et al, 2011). It is unclear how the paradigm-shaping literature developed in different biophysical regions apply to low-relief glaciated regions found in central North America and Eurasia, where hydrologic functioning differs substantially in part due to differences in soil moisture storage, wetland extent, and groundwater exchange.

Studies on the effects of forests on streamflow have historically focused on catchment spatial scales of < 10 km$^2$ (Stednick, 1996;  Andréassian, 2004; Hewlett et al., 1969; Likens, 2001; Loftis et al., 2001). In particular, "detectability thresholds" derived from the traditional paired catchment literature have unclear application to larger basins where cumulative forest disturbances occur over several years (Wei et al., 2021).  Experimental catchments are specifically designed with statistical requirements for the

attribution of causal mechanisms in mind, which rely on small, relatively homogeneous catchments. However, at larger spatial scales where landscapes are heterogeneous and data collection networks are less dense, there are difficulties in applying empirical approaches.

At larger catchment scales, different streamflow generation processes may emerge compared to the headwaters catchments on which the catchment science literature focuses (Blöschl, 2022; Blöschl et al., 2007; Rogger et al., 2017). Emergent properties of streamflow generation at large scales include the importance of regional groundwater, increasing catchment heterogeneity, catchment storage and channel routing processes, and the importance of large-scale climate variability (Laudon and Sponseller, 2018; Viglione et al., 2016). As catchments scale up in size, structure and function of relevant flow-generating units in the catchment can shift. For example, heterogeneity in catchment structure and physical characteristics, such as surficial geologic deposits, increases with catchment area. Catchments large enough to include multiple geologic units often have areas of disproportional hydrologic function at the boundaries of different deposits (e.g., flow along fault lines: Bense et al., 2013). Additionally, climate variability is expected to be a dominant signal in large as opposed to small (e.g. headwater) catchments (Rogger et al., 2017). Because structure and other drivers differ, there is a need to conduct studies in large catchments instead of inferring large catchment responses from previously conducted small catchment studies.

Empirical approaches are commonly used to assess the effects of forest disturbance on streamflow processes, allowing for the testing of hypotheses not constrained by an *a priori* conception of the physical processes at work. Many studies have utilized the Before-After-Control-Impact (BACI) design (Andréassian, 2004; Hewlett et al., 1969; Neary, 2016). Regression analysis, nonparametric tests, and timeseries analysis have been used to empirically test for streamflow response to harvesting in large catchments (Hou et al., 2022; Jones & Grant, 1996; Lin & Wei, 2008). A key step in these types of analyses is the quantification of cumulative forest disturbance, which serves as the independent variable to assess the cumulative effect of many small disturbance events over time. Associated with this approach is the concept of "hydrological recovery" which is the time period required for the disturbed portion of

the catchment to function similar to its pre-disturbance condition. Estimating hydrologic recovery time has been approached by using: 1) considerations from silviculture (e.g., when does that species of tree exceed a certain maturity threshold?) (Giles-Hansen et al., 2019; Lin & Wei, 2008), 2) the pairing of catchments and assessing based on relative disturbance intensity (Jones & Grant, 1996), and 3) past empirical paired-catchment results to constrain recovery time (McEachran et al., 2021). Alternative approaches include controlled plot-scale studies (Pierson et al., 2007), meta-analysis of catchment studies across regions (Ali et al., 2015), and using models, either physically-based, statistical, or their combination (Zégre et al., 2010). The ability to generate long synthetic streamflow records is a key advantage of modeling-based studies (Green & Alila, 2012), but the use of empirical data still offers a distinct advantage in its lack of reliance on a particular physical-science paradigm, and complements modeling studies as validation and advancement of the physical paradigms used in process-based models.

In this paper, we utilize probabilistic approaches to empirically assess the effect of forest disturbance on water yield and peak streamflow at a range of catchment sizes in the low-relief, glaciated Minnesota, USA. We investigated the hypothesis that forest cover loss through harvesting and/or fire results in increased water yield and increased peak streamflow, and that discernible signals of spatial scale are detectable in the relationship of streamflow to forest disturbance across catchments 50-9000 km$^2$.

## 2. Methods

### 2.1: Study Area

#### 2.1.1: Upper Kawishiwi Basin.

The Kawishiwi River starts in a small lake in the Hudson Bay drainage, and flows entirely on the southern Canadian Shield. The Upper Kawishiwi Basin has an area of 650 square kilometers, and is almost completely in the Boundary Waters Canoe Area Wilderness. The catchment has thus been largely protected from development since 1964. In August of 2011, a lightning strike ignited the Pagami Creek Fire, and burned 27% of the catchment area (200 sq km) (Figure 1).

Crystalline bedrock is often <1 m from the soil surface (Jirsa et al., 2011), although deeper peat deposits and deep lakes in bedrock depressions are common. Soils are generally coarse-textured, but perched wetlands over lacustrine clay confining layers are common (Prettyman, 1978). Approximately 29% of the watershed area in the Upper Kawishiwi Basin comprises lakes and wetlands (Minnesota National Wetlands Inventory, 2019), with ~13% of the watershed area in open-water storage. In-channel lakes constitute 82% of the channel length of the Kawishiwi River (Minnesota Department of Natural Resources, 2022). The Upper Kawishiwi catchment was 83% forested before the fire, with mostly evergreen and woody wetland forest types (28% and 24%, respectively) (NLCD 2011: Homer et al., 2015). The climate in the Upper Kawishiwi catchment is continental, with moist warm summers and dry, cold winters. Since 1895, the average annual precipitation is 693 mm, about 27% of which occurs in the winter largely as snow (PRISM Climate Group, 2020).

*2.1.2: St. Louis River Basin.*

The St. Louis River begins in a region of shallow lakes and peatlands, and flows through extensive glacial deposits before draining into Lake Superior in Duluth, Minnesota (Figure 1). It is the largest river to drain into the Great Lakes, with a drainage area of 8,880 km$^2$ at the most downstream gage at Scanlon, Minnesota. The St. Louis River flows through material of multiple glacial provenances, intersecting with areas of glacial lake, till plain, morainal, and drumlin landforms (Hobbs and Goebel, 1982). A large portion of the basin is wetlands (60% of the area at the Scanlon gage) particularly where lacustrine sediments constitute the parent material (Figure 1). There are few open-water lakes in the catchment, in contrast to the Kawishiwi catchment. All catchments contain about 1/3 upland forest and ~50% woody wetlands (2019 NLCD: Dewitz and USGS, 2021). Mining land use is common in the northern portion of the basin, but land use/land cover has not changed substantially since the formal NLCD record began in 2001, indicating largely stationary non-forest land cover patterns at the basin

scale. Primary disturbances were broadly distributed and associated with a patchwork on the scale of <1 km² per disturbance.

### 2.2: Data Sources and Aggregation

We used two contrasting case studies to investigate how forest disturbance affects water yield and annual maximum peak flows. First, the Upper Kawishiwi River catchment (Figure 1) was a single catchment analyzed over a 53 year time period with a wildfire that burned ~1/3 of the catchment area. Second, the St. Louis River Basin case study involved 11 catchments, some of which were nested, over a shorter period of time (Figure 1; Table 1). The two case studies were used to assess the effect of forest disturbance on streamflow for two common disturbance regimes: in the Kawishiwi, a rapid and large-scale disturbance over a large area, and for the St. Louis, a patchwork cumulative disturbance of various sources, but mostly forest harvesting.

Published streamflow records were compiled from federal and state government agencies. The Kawishiwi case study utilized daily flow records from a United States Geological Survey (USGS) gage (USGS 05124480) from 1967-2019. The St. Louis River Basin case study used data from 11 gages managed by USGS, the Minnesota Department of Natural Resources, and Minnesota Pollution Control Agency, collectively housed at the Minnesota Cooperative Streamgaging Network (https://www.dnr.state.mn.us/waters/csg/index.html; Last accessed January, 2022). Gages within the St. Louis utilized available data from 1986-2018. Daily streamflow records were used when available, while sub-daily streamflow records were converted to daily records using standard numerical methods (see Supplemental Section 1 for data processing notes). Catchments for each gage location (Table 1) were delineated using Streamstats v.4 (USGS, 2016), which relies on a 10 m elevation model to delineate catchment boundaries.

We defined a streamflow water year as between March and February of the next year after Sebestyen et al. (2011). This definition encapsulates streamflow seasonality in northern climates, which is

greatly reduced in winter and starts to increase with early spring warming in March. We defined the water year for all non-streamflow variables (such as precipitation) as between November and October of the following year (also as per Sebestyen et al., 2011), to reflect the contribution of snowpack to the streamflow water year. Winter was defined as November through April, and spring was defined as May through June, based on snowpack trends at the Winton, MN NOAA weather station (NOAA-NCEI, 2020; Menne et al., 2012a; Menne et al., 2012b). Regional maximum flows are most often either the spring freshet, or the result of spring rains on a saturated catchment in late spring or early summer; summer rainstorms occasionally produce annual maximums (McEachran et al., 2021).

Meteorological data were derived from Oregon State's PRISM database of monthly values (4km resolution; PRISM Climate Group, 2020) and aggregated across a 1 km raster cell resampling of the catchment, either through addition (summing annual, winter, and spring precipitation), or averaging across the entire year (temperature, dew point, etc.). The meteorological variables used to analyze annual water yield and peak flows can be found in Table 2, in addition to using large-scale climatic indices (namely, the Atlantic Multidecadal Oscillation).

Two Minnesota forest disturbance data sources were used for the St. Louis analysis: a single map layer representing the "Most Recent Fast Forest Disturbance" for a given area, wherein forest patches that had been detected as disturbed at any time in 1975-2018 were identified with the year of their most recent disturbance (Vogeler et al., 2020; Vogeler, 2019), and an additional set of annual forest disturbance maps spanning 1986-2018 (unpublished data, J. Vogeler). Disturbance pixels were identified using the Landsat time series trend fitting algorithm, LandTrendr (Kennedy et al., 2010), grouped into change patches representing a shared change event, and then classified by disturbance agent using random forest modeling. The random forest agent attribution model was trained on a set of patches where the disturbance agent was known through photo-interpretations, local knowledge, field visits, or additional spatial data sets (e.g., Monitoring Trends in Burn Severity). Disturbance categories were aggregated as "regenerating" and "permanent" (i.e., conversion) for the purposes of the hydrologic analysis. Regenerating disturbances included stand change categories of harvest, windthrow, fire, and other.

Because of the possibility of patches being disturbed more than once in the period of record, the annual maps were used for the extent of their record. The annual maps were produced using similar Landsat time series change detection and patch attribution approaches as presented in Vogeler et al. (2020) across the state of Minnesota, with the exception that changes were identified on an annual basis from the time series as opposed to focusing only on the most recent event for a given area, and only included the Landsat data beginning in 1984 (with change maps starting in 1986). The most recent change map included information from the early Landsat MSS sensors which require additional pre-processing and calibration to incorporate with the rest of the Landsat archive that begins in 1984 (Vogeler et al., 2020). The longer-running "most recent" map product was used to fill in data 1975-1985. To explore potential recovery time for forest disturbances ranging between 1 and 20 years, we extrapolated the most recent forest disturbance map product back to 1967, with 1967-1975 being set equal to the mean annual regenerating disturbance within the first 15 years of the most recent fast forest disturbance layer. At the catchment scale we created an aggregated "disturbed" metric with the percentage of catchment area disturbed by a regenerating forest disturbance in a given year (plus N prior years within a recovery window). Forest conversion was added to the annual catchment-scale "disturbed" metric as a cumulative sum of areal percentage converted since 1986 (year 1 of water yield modeling where there was streamgage data, and of the annual forest disturbance mapping product). This representation of disturbance assumes all converted forest, and regenerating disturbance before the recovery year, behaves differently than pre-disturbance with respect to hydrology; once the recovery year is met, that formerly disturbed patch returns to the pre-disturbance hydrological baseline (for non-conversion disturbances). Thus, in 1986, the 1-year forest disturbance metric includes the regenerating forest disturbance that occurred in 1986, plus the conversion that occurred in 1986. In 1990, the 11-year forest disturbance metric included the sum of the regenerating forest disturbance that occurred in 1980-1990, plus the cumulative forest conversion that had occurred since 1986. Total forest conversion in the basins was low, with a basin maximum annual conversion rate of 0.25% of basin area, and a maximum cumulative sum

(1986-2018) of 1.56% of basin area. This compares to the regenerating forest disturbance maximum

annual value of 2.38% in a single year. Finally, the rest of the landscape was treated as stationary.

*2.3: Modeling Methods*

Our overarching modeling approach uses linear models for water yield and peak flows, in addition to

probabilistic flood-frequency models for peak flows. Linear modeling approaches are commonly used to

assess the effect of forest disturbance on water yield and peak flows (Jones & Grant, 1996; Lin & Wei,

2008). However, recent literature has shown the importance of also analyzing peak flows using

probabilistic flood-frequency frameworks to draw inferences about how forest disturbance and climate

factors influence the peak flow at particular return intervals (Alila et al., 2009; McEachran et al., 2021).

The modeling workflow is outlined in Figure 2. The first step in each analysis was data exploration and

variable selection. More detailed information on variable selection and modeling approach can be found

in Supplemental Section 2; manual and automated techniques were both used. The general approach for

the Kawishiwi basin was to first model the pre-fire streamflow using climate variables alone, then

compare the actual observed streamflow with the predicted streamflow after the fire based on the pre-fire

models. This process included selecting climate variables using manual techniques and then analyzing

water yield and peak flows using a linear model. Peak flows were also modeled in a nonstationary flood-

frequency analysis, the structure of which was chosen via formal/automated model selection. For the St.

Louis basin analysis, climate effects on water yield and peak flows were assessed using five to six

candidate Linear Mixed Effects (LME) models per streamflow variable. LME was used because of

catchments' biophysical similarity, while allowing a unique response to climate drivers for each

catchment. The "fixed effect" represented an overall region-specific mean effect of the climate driver on

streamflow, while the "random effect" allowed each basin to modify the fixed effect according to its

specific hydrologic response to that climate driver. Manual variable selection informed the candidate

LMEs, with the final LME chosen using automated selection. The streamflow residuals from the selected

best-fit LME, representing climate-detrended streamflow, were then modeled with forest disturbance as a

linear predictor. Detrending a variable by using the residuals from a regression analysis is a common

practice (Iler et al., 2017), and modeling the climate-only variability in streamflow first ensures no

multicollinearity with forest disturbance predictors when those are modeled based on the climate-only

residuals. This is a conservative choice with respect to our hypotheses insofar as any collinearity between

climate and forest disturbance is attributed to climate drivers. Peak flows in the St. Louis basin were also

analyzed in a nonstationary flood-frequency framework that parsed the peak flow distribution into

stationary and nonstationary components; from this flood-frequency model, we obtained the annual

maximum peak flow with a 50% annual exceedance probability (the Q2). We then modeled the

nonstationary component of the Q2 with climate and forest disturbance predictors. The Q2 was chosen

because it is critical for the average channel-forming flow for alluvial river systems (Wolman and Miller,

1960; Phillips and Jerolmack, 2016), and streamflow records were <5 years in some basins.

For all models, we used Bayesian-based Markov chain Monte Carlo (McMC) sampling (Gelman

and Rubin, 1992) to generate a full probabilistic estimate for the parameters conditioned on the observed

annual water yield and annual maximum flow, except where explicitly stated. For the McMC sampling,

we implemented the JAGS ("Just Another Gibbs Sampler") algorithm (Plummer, 2003) with the "R2jags"

package (Su and Yajima, 2015) in R (R Core Team, 2022). We used noninformative priors, including

normal distributions with wide standard deviations, or uniform distributions where parameters were

defined only when greater than zero. Model appropriateness was assessed by visually inspecting residuals

versus fitted and normal QQ plots, and posterior-predictive checks (Gelman et al., 1996). We reported the

confidence we have for an hypothesized positive or negative relationship between streamflow and forest

disturbance as represented by the sign (+/-) of "effects" parameters within the models, based on their

modeled posterior density distributions (Gelman and Tuerlinckx, 2000). There is no strict threshold for

"significance", but rather our confidence is the weight of evidence corresponding to an effect parameter

of forest disturbance on streamflow as being positive or negative (McShane et al., 2019). While we

consider confidence to be a continuous quantity, where hypotheses have ~10:1 odds in favor (which is

where we would be 91% confident), they are often considered to have substantial to strong support (Kass

and Rafferty, 1995), so we consider >90% confidence as "high confidence" effects. Finally, for all models, McMC convergence was supported by the Gelman-Rubin statistic and visual inspection of traceplots.

*2.3.1: Upper Kawishiwi Methods*

Before the fire (2011), we selected the annual precipitation and the annual average monthly Atlantic Multidecadal Oscillation (AMO) index as the dominant climate drivers of streamflow in the Upper Kawishiwi catchment, after selecting for variables shown in Table 2 and assessing spectral trends in the hydrometerological data using the Fast Fourier Transform (NOAA – PSL, 2020; Supplemental Section 2). There was also a clear piecewise change point at AMO = 0, consistent with regional literature (Mengistu et al., 2013). Thus, the effects of the 2011 fire on water yield were assessed with respect to Equation 1:

$$Q_i = b_0 + b_1 * P_i + b_2 * AMO_i + b_3 * \alpha_i + b_4 * AMO_i * \alpha_i + \varepsilon_i \tag{1}$$

$$\varepsilon_i \sim Normal(0, \sigma^2)$$

Where $Q_i$ is the annual water yield in year $i$ [mm], $P_i$ is the annual precipitation in year $i$ [mm], $AMO_i$ is the annual average monthly AMO index value in year $i$ [dimensionless], and $\alpha_i = 0$ when $AMO_i \leq 0$ and $\alpha_i = 1$ when $AMO_i > 0$. For the annual maximum flow regression, we utilized Equation 1, but $Q_i$ represented the annual maximum streamflow, and $P_i$ represented the winter precipitation.

Each year $j$ after the fire (2012-2019), we sampled the distribution of expected $Q_j$ based on that year's climate forcings by sampling the posterior densities of the regression parameters and the error term $\varepsilon_i$. The proportion of the distribution of expected $Q_j$ values in each year below the observed value was our confidence that water yield increased more than would be expected after the fire.

The probabilistic flood-frequency approach for annual maximum flow utilized the same driving climate variables used in the regression analysis. We used the Gumbel distribution (Gumbel, 1958; Lima and Lall, 2010) to describe the annual maximum streamflow. The Gumbel distribution is parameterized by a location (μ) and scale (σ), which were modeled linearly by winter precipitation and AMO index in a nonstationary framework. After fitting models for all combinations of linear dependence of location and scale on winter precipitation and AMO index, Equation 2 was chosen as the most probable model for the 1967-2011 time period (degree-of-belief = 0.339) (Supplemental Table 3.1).

$$Q_{max,i} \sim Gumbel\ (\ \mu_i\ ,\sigma_i\ ) \tag{2}$$

$$\mu_i = a_1 + a_2 * AMO_i + a_3 * P_i$$

$$\sigma_i = \sigma_{prefire}$$

In Equation 2, $Q_{max,i}$ is the annual maximum daily discharge in pre-fire year $i$; $\mu_i$ and $\sigma_i$ are the location and scale parameters in year $i$, respectively; $\sigma_{prefire}$ is the stationary pre-fire scale parameter; $a_1$, $a_2$, and $a_3$ are hyperparameters describing how $\mu_i$ varies with AMO and winter precipitation; and $P_i$ is the winter precipitation in year $i$.

To assess the effect of the fire, we added constant effects hyperparameters to allow the fire to impact peak flows either through the location, scale, or both parameters (Equation 3):

$$Q_{max,j} \sim Gumbel\ (\ \mu_j\ ,\sigma_j\ ) \tag{3}$$

$$\mu_j = a_1 + a_2 * AMO_j + a_3 * P_j + \mu_o$$

$$\sigma_j = \sigma_{prefire} + \sigma_o$$

In equation 3, variables remain the same as in 2, except for the year indexing which is over post-fire years $j$, and the constant effects hyperparameters $\mu_o$ and $\sigma_o$, which represent the changes to the location and scale parameters due to the fire, respectively. Cumulative Distribution Functions (CDFs) through the 2% exceedance probability were compared when the effects hyperparameters were set to zero, versus allowed to be non-zero in Equation 3.5, representing "expected" and "treated" conditions, respectively. We chose the 2% exceedance probability because the approximate level of information we have from the system was commensurate with the 2% exceedance probability event (i.e., ~50 years of data).

*2.3.2: St. Louis Methods*

**2.3.2.1: Linear Mixed Effects and Linear Regression Analysis**

We selected the water yield candidate regressions through considering the pooled correlation matrix on all streamflow data in the basin, water balance considerations, and the results from the Kawishiwi analysis (Supplemental Table 2.1). Because of multicollinearity between many of the predictors, we also used the first principal component of the ET-driving variables as a possible predictor (see Table 2 for details).

$$yield_{i,j} = annual\ water\ yield\ in\ year\ i\ in\ catchment\ j$$

$$yield_{i,j} = Normal(\hat{q}_{i,j,s}, \sigma_s)$$

$$\hat{q}_{i,j,1} = \left(b_{0,1} + bc_{0,j,1}\right) + \left(b_{1,1} + bc_{1,j,1}\right) * P_i$$

$$\hat{q}_{i,j,2} = \left(b_{0,2} + bc_{0,j,2}\right) + \left(b_{1,2} + bc_{1,j,2}\right) * P_i + \left(b_{2,2} + bc_{2,j,2}\right) * VPD_i$$

$$\hat{q}_{i,j,3} = \left(b_{0,3} + bc_{0,j,3}\right) + \left(b_{1,3} + bc_{1,j,3}\right) * P_i + \left(b_{2,3} + bc_{2,j,3}\right) * PET_i \qquad (4)$$

$$\hat{q}_{i,j,4} = \left(b_{0,2} + bc_{0,j,2}\right) + \left(b_{1,2} + bc_{1,j,2}\right) * P_i + b_{2,4} * AMO_i + ba_0 * \alpha_i + ba_1 * \alpha_i * AMO_i$$

$$\hat{q}_{i,j,5} = \left(b_{0,5} + bc_{0,j,5}\right) + \left(b_{1,5} + bc_{1,j,5}\right) * P_i + \left(b_{2,5} + bc_{2,j,5}\right) * ET.PCA1_i$$

$$s \sim Categorical(5; \ p_1, \dots, p_5)$$

In Equation 4, the $b$'s are fixed effects, $b_c$'s are random (catchment) effects, and σ is pooled model variance. The other climate variables are annual aggregations of the variables in Table 2. The AMO model was a breakpoint regression as in the Kawishiwi regressions. The selected final model $s$ was that which had the highest probability $p_s$ after conditioning on the data.

The candidate LMEs for peak flows had the same structure as Equation 4, but with different terms, with predictors of 1) spring precipitation only, 2) winter precipitation and spring precipitation (no interaction), 3) spring precipitation plus winter/spring precipitation interaction, 4) spring precipitation plus AMO index as in the Kawishiwi regression, 5) spring precipitation and fall precipitation, and 6) spring precipitation, and winter precipitation and winter mean temperature interaction (Supplemental Table 2.2). These candidate variables were selected due to considering the overall correlation matrix, and considering the dominant mechanisms of regional flooding as rapidly melting snowpack or rain-on-snow in the spring after a wet fall (Verry et al., 1983). Additional rationale for each candidate model is given in Supplemental Table 2.2, and the equations are written out explicitly in Supplemental Equation 2.1. We divided each annual maximum streamflow (m$^3$/s) by 100 times each basin's area to get a per-area value (m$^3$/s per 100 km$^2$) so we could pool residual variance across catchments and to support McMC convergence.

The residuals from the best-fit climate-only LME, at the mean posterior density for the parameters and with the highest $p_s$ (Equation 4) were then modeled with forest disturbance as a linear predictor. To incorporate recovery, 20 regressions were fit with recovery year ranging from 1 to 20 years.

$$r_{i,j}$$
$$= unexplained\ portion\ of\ water\ yield\ or\ peak\ flow\ after\ accounting$$
$$for\ climate\ factors\ in\ \hat{q}_{i,j,s}\ in\ year\ i\ in\ catchment\ j \qquad (5)$$
$$r_{i,j} \sim Normal(\widehat{r_{i,j,N}}, \sigma)$$
$$\widehat{r_{i,J,1}} = br_{0,1} + br_{1,1} * d_{i,j,1}$$

$$\widehat{r_{i,j,2}} = br_{0,2} + br_{1,2} * d_{i,j,2}$$

$$...$$

$$\widehat{r_{i,j,20}} = br_{0,20} + br_{1,20} * d_{i,j,20}$$

$$\widehat{r_{i,j,N}} \sim Categorical(20; \ p_1, p_2, \ldots, p_{20})$$

Where $\widehat{r_{i,j,N}}$ is the expected climate-detrended water yield or peak flow in year $i$ in catchment $j$ with a

forest recovery time of $N$ years, with $d_{i,j,R}$ representing forest disturbance in year $i$ in catchment $j$ with a

recovery time of $R$ ranging from 1 to 20 years. The highest $p_N$ represents the most-likely recovery year $N$.

Our confidence in the sign of $b_{1,N}$ (i.e., X% confidence that $b_{1,N} > 0$) represents our confidence in an

effect.

**2.3.2.2: Probabilistic analysis of annual maximum streamflow**

We used a nonstationary Gumbel model for annual maximum streamflow (Lima and Lall, 2010).

The location and scale parameters had a stationary mean determined by basin spatial scale: both

parameters of the Gumbel distribution increase linearly in log-log space with spatial scale (Lima and Lall,

2010; Equation 6). We also allowed the location and scale to vary year-to-year, thus incorporating

potential nonstationarities (Lima and Lall, 2010). Thus, the location and scale parameters of the Gumbel

distribution, as modeled, are comprised of 1) a stationary component determined solely by the log-log

scaling of these parameters with basin spatial scale, and 2) a nonstationary component determined by the

annual variability of these parameters, varying according to some variance $\sigma^2$.

$$mx_{i,j} = annual \ maximum \ streamflow \ in \ water \ year \ i \ in \ catchment \ j$$

$$mx_{i,j} \sim Gumbel\left( lo_{i,j}, sc_{i,j} \right)$$

(6)

$$\ln\left(lo_{i,j}\right) \sim \text{Normal}\left(b_0 + b_1 * x_j , \sigma_{lo}\right)$$

$$\ln(sc_{i,j}) \sim \text{Normal}\left(b_2 + b_3 * x_j, \sigma_{sc}\right)$$

$$\overline{q_{2_{i,j}}} = lo_{i,j} - sc_{i,j} * \ln(-\ln(0.5))$$

$$\overline{stat.q_{2_j}} = (b_0 + b_1 * x_j) - (b_2 + b_3 * x_j) * \ln(-\ln(0.5))$$

Following Lima and Lall (2010), we transformed our catchment sizes to a zero-mean predictor to facilitate model convergence. The Q2 was estimated using the quantile function of the Gumbel distribution at a quantile of 0.5, which is defined as lo – sc*ln(-ln(0.5)). Thus, the stationary Q2 is the 50% quantile of the Gumbel distribution defined by the log-log scaling regression of the location and scale parameter that only relies on the basin spatial size. In addition to this, in each individual year, the Q2 "randomly" varies according to some variance of the location and scale parameters. However, because Bayesian parameter estimation is used, we can actually estimate the value of the Q2 in those years (Lima and Lall, 2010). Thus, we can compare the actual best-estimate Q2 in each individual year against what would have been predicted as the Q2 in the absence of the nonstationary variability. The difference between $\overline{q_{2_{i,j}}}$ (the nonstationary q2) and $\overline{stat.q_{2_j}}$ (the stationary q2 determined solely by catchment size) represented the component of the Q2 attributable to nonstationary processes. We modeled the mean posterior density value of the nonstationary component of the Q2 against forest disturbance and a winter/spring precipitation interaction using a linear model. We chose the winter/spring interaction term because of a correlation analysis, the results of the peak flow LMEs, and attempting to encapsulate the key peak flow drivers of the region in a single variable (Verry et al., 1983).

$$diff.q2_{i,j} = \overline{q_{2_{i,j}}} - \overline{stat.q_{2_j}} \tag{7}$$

$$diff.q2_{i,j} \sim \text{Normal} \left( \left( a_{0,j} + a_{1,j} * dist_{i,j} + a_{2,j} * ws.precip_{i,j} \right), \sigma_j \right)$$

Where $dist_{i,j}$ is the N-year forest disturbance that was selected in the peak flow LME analysis, $ws.precip_{i,j}$ is the winter precipitation multiplied by spring precipitation, centered on the mean and divided by standard deviation to align the magnitude of variability with forest disturbance, and in year $i$ in catchment $j$, $a$'s are regression parameters, and $\sigma_j$ is a catchment-specific standard deviation. The sign of the effect hyperparameter $a_1$ was assessed as direction of the effect of forest disturbance on the Q2. Finally, to assess how much overall variability in the Q2 is explainable by nonstationary processes, we compared the mean ratio of the magnitude of $diff.q2_{i,j}$ to $\overline{q_{2_{i,j}}}$ for each catchment. Because some years the Q2 is lower than that expected due to stationary processes alone, and some years it is higher (and thus can "cancel out" the overall magnitude of nonstationarity), to assess the relative importance of stationary versus nonstationary drivers, we took the root squared difference between the nonstationary and stationary Q2 components as the magnitude of the nonstationary effect, and compared this to the overall magnitude of the Q2.

## 3. Results

### 3.1: Kawishiwi

Expected and observed water yield after the fire are shown in Table 3. Water yield was elevated in years 2-6 after the fire. In all eight post-fire years, the climate variables accounted for 58% of the variability in water yield. There were only three years where water yield increased more than 10 mm after the fire (years 2-4). We were >90% confident in this effect in year two, 83% confident in year three, and

≤ 80% confident in both yield increases or yield decreases in all other post-fire years. Water yield recovered to pre-fire conditions within 5 years of the fire: the hydrologic effect of fire to surface water was short-lived compared to the regional guidelines of 15-year hydrologic recovery after forest harvesting disturbance.

The regression results for annual maximum flow showed no increases or decreases for which we were greater than 90% confident (Table 4). However, we were 88% confident that the annual maximum flow increased in year 3 after the fire, and 86% confident that the annual maximum flow decreased in year 5 after the fire. Overall, the annual maximum flow regression gave lower confidence for any fire effects, and a lack of consistent effect direction, if one existed. The dominance of climate factors is also apparent via the regression results for annual maximum flows. The winter precipitation and AMO index accounted for 32% of the variability in post-fire annual maximum flows. Although this is less than one half, annual maximum flows were much more variable even in the pre-fire time period, with a residual standard error of 1.1 mm/day. The climate variables were even better predictors in describing post-fire annual maximum discharges than during the pre-fire years: after the fire, the residual standard error between the predicted values and the observed values according to the ANCOVA had a residual standard error of 0.80 mm/day. Despite this variability, climate trends via winter precipitation and AMO index were detectable and significant for describing the annual maximum flow, while the 2011 fire was not a detectable signal (with confidence) in the annual maximum flow series.

There was no effect for which we were confident of the fire on Gumbel distribution location or scale parameters ($\mu_o$ = -0.10 ± 0.35 (p = 0.62); $\sigma_o$ = -0.13 ± 0.31 (p = 0.72)). We found no changes in the annual maximum daily streamflow in any year for which we were greater than 80% confident across the entire CDF, from the 2-year to 50-year return interval event (i.e., all Type-S p > 0.20). Annual maximum flows at any given return interval actually *decreased* relative to what we would expect based on the pre-fire predictions, but with low (<80%) confidence. Climatic drivers were much more apparent than fire effects for peak flows in the frequency analysis as well: while the effect of the fire on the location parameter for the Gumbel distribution was -0.10, a change in the AMO index of one standard deviation of

that observed 1967-2019 changed the location parameter by 0.33. In a year with average winter precipitation (195 mm), and the AMO is at the minimum observed 1967-2019, the 1.5-year annual maximum flow is 3.5 mm/day, versus when AMO is at a maximum it is 2.2 mm/day, causing a difference of over 1 mm/day (> 50% difference). However, when the AMO is at its mean value for 1967-2019, as is winter precipitation, the 1.5-year flow on the burned catchment is 2.7 mm/day, versus an expected (i.e., projected based on pre-fire relationships) 2.8 mm/day, a difference of only approximately -4%.

### 3.2: St Louis Results

Of the five potential equations for water yield from Equation 4, the equation including both precipitation and the first ET-principal component was chosen in 92% of samples, indicating a high degree of belief that this was the best climate-only model. This model had the highest $r^2$ value (0.79) and lowest standard residual error (41mm). The "fixed effect" runoff ratio, or mm of water yield per additional mm of precipitation, was $0.69 \pm 0.11$; all precipitation parameters were greater than 0 (Type S $p < 0.001$). The first ET principal component fixed effect was inversely correlated with water yield – as factors that increase ET (vapor pressure deficit, PET, etc.) increased, water yield decreased. However, confidence in this relationship was generally low ($p = 0.33$). Other fixed effects parameters for the selected model are available in Supplemental Table 3.2. Precipitation was the dominant explanatory variable in the regression, with a precipitation-only regression having an $r^2$ of 0.70.

The recovery time for the effect of forest disturbance on climate-detrended water yield was 11 years (Figure 3). We were ~9.3 times more confident that when a forest disturbance occurred and was allowed to regenerate, that forest returned to a pre-disturbance impact on water yield in 10 or 11 years, rather than any other recovery year window between 1 and 20 years. The effect of the 11-year forest disturbance on climate-adjusted annual water yield is shown in Table 5. A majority of catchments did not show water yield changing substantially in response to forest disturbance (8 of 11 catchments had

confidence of effect < 90%). For three of the 11 catchments, including the smallest and largest catchments, we were >99% confident that increasing the proportion of forest that was disturbed within the previous 11 years was associated with lower climate-detrended water yield. For each additional percentage of the basin that had been disturbed within the previous 11 years, water yield decreased 5 to 25 mm (including the 90% credible interval), depending on the basin (Table 5). Size of the disturbance effect was inversely related to basin size where we were >90% confident in the effect. However, the amount of overall variability explained by forest disturbance was low. While the climate-only model of water yield had an $r^2$ of 0.79, the $r^2$ of the regression of climate-detrended water yield versus 11-year forest disturbance was 0.13. Thus, the variability of the overall water yield that may be attributable to forest disturbance was ~3%, as only 21% of the variability in water yield remained after controlling for the climate, and 13% of that was attributable to forest disturbance.

For peak flows, the spring precipitation plus winter precipitation and winter temperature interaction model was chosen 99% of the time. This model had an $R^2$ of 0.63, and a residual standard error of 2.1 [$m^3$/s / 100 $km^2$]. However, the parameters had much higher uncertainty compared to the water yield model, with none of the fixed effect parameters being greater than or less than zero with any confidence (Type S p's ~ 0.5). Other fixed effects parameters for the selected model are available in Supplemental Table 3.3. The best-choice forest recovery model of the climate-detrended peak flows was 13 years of forest disturbance (Figure 4). Using the 13-year recovery model, forest disturbance was positively or negatively correlated with climate-detrended annual maximum streamflow residuals in four of the 11 basins with >90% confidence (Table 6). There was no consistent directionality for an effect, with two catchments showing a negative correlation, and two catchments a positive correlation. However, the 13-year forest disturbance only explained 22% of the variance of the climate-detrended peak flows and peak flows still had a residual error of 1.8 [$m^3$/s / 100 $km^2$]. Therefore, of the remaining 37% of the variability in peak flows remaining after climate detrending, 22% of that was explained by forest disturbance variables. This portion, then, totals 8% of the variability in peak flows explained by forest

disturbance. The forest disturbance only contributed 0.3 [$m^3$/s / 100 $km^2$] more information to the peak flow estimation of the model.

The 13-year forest disturbance and winter*spring precipitation explained 44% of the variability in the nonstationary component of the Q2, with effects hyperparameters shown in Table 7. The St Louis River near Forbes (1791 $km^2$) indicated that as 13-year forest disturbance increased, the expected Q2 actually *decreased* (confidence = 98%). Furthermore, in all basins, when the winter*spring precipitation increased, the Q2 also increased with >90% confidence in 5 of 11 basins. The magnitude of the annual nonstationary fluctuations in the Q2 comprised 20% of the overall Q2 estimate (Figure 5). This means that changing land cover and changing climate variables in the 1986-2018 time period, even if significantly affecting the Q2, only could influence up to 20% of the relative magnitude of the Q2. The remaining variability in Q2 basin-to-basin was solely modeled via scaling its basin parameters according to basin spatial scale. Of this unexplained variation in Q2 year-to-year, the winter*spring precipitation term explains 49% of the variability if the forest disturbance is held at the mean level, while if the winter*spring precipitation is held at its mean level, the forest disturbance term only explains 2% of the variability in nonstationary Q2. Thus, climate and basin spatial scale have a substantially higher impact on Q2 at these scales.

## 4. Discussion

Forest disturbance had a discernible correlation with water yield in both case studies, but in different directions. In the Kawishiwi, forest disturbance was associated with a water yield increase (30% increase maximum), but this effect disappeared after 5 years, and we were only >90% confident of an effect existing in year 2 after the fire. In the St. Louis Basin, we observed that more forest disturbance was associated with a water yield decline compared to what was expected based on climate alone

(accounting for uncertainty, between -10% and -2% of the basin mean water yield for each percentage point of additional forest disturbance within the previous 11 years). Effects of forest disturbance on annual maximum peak streamflows were mixed, with some increases and some decreases observed. Catchments in the boreal-temperate transition zone have high storage capacity which may attenuate effects of forest disturbance on peak flows.

*4.1: Disturbance Type, Recovery Time, and Streamflow Effects*

Differences in disturbance regime influenced the effects of forest disturbance on streamflow. The Kawishiwi case study focused on a "catastrophic" forest disturbance regime, in which a large portion (~30%) of a catchment was deforested by fire within a single year. The foundational paradigm in which "forest disturbance increases water yield" is largely based on stand-clearing forest harvesting experiments at the small catchment scale (Brown et al., 2005; Stednick, 1996; Bosch and Hewlett, 1982). The Kawishiwi case study represented an analogue to this approach but at a larger scale, and our results were consistent with the literature (e.g., the response plots well within Buttle 2011: Figure 33.1a). However, the effect decayed more rapidly than in small catchment studies in the region (e.g., Sebestyen et al., 2011). Furthermore, the temporal pattern of the effect indicated basin scaling and storage impacts on streamflow unique to large catchments (discussed in Section 4.2).

When more disturbance types were considered across multiple years (i.e., the St. Louis case study), however, we found that more disturbance was associated with lower water yield. This disturbance measure was focused on a distributed multi-year aggregation of harvesting, fire, conversion, and windthrow. There is a growing catchment sciences literature examining the effect of incremental disturbances that do not clear the entire canopy in a single event (Bart et al., 2021; Goeking & Tarboton, 2020; Brantley et al., 2013). Forest disturbance, especially at sub-catchment scales, has been shown to reduce water yield due to compensatory evapotranspiration (ET) from other, nearby, trees and undergrowth vegetation or higher ET rates in disturbed areas arising from vigorous early regeneration,

increased surface evaporation, or increased ET by remaining species when a forest is thinned but not cleared (Goeking & Tarboton, 2020; Bart et al., 2021; Segura et al., 2020). In a recent review of the literature from western North America focusing on widespread tree mortality occurring after the year 2000, non-stand-replacing disturbance was more likely to have been associated with a decrease in water yield compared to stand-replacing disturbance (Goeking & Tarboton, 2020). In Minnesota, rapid regrowth of young aspen (*Populus* spp.), common in the St. Louis catchments, has been documented as vigorous, with 2m+ tall sucker growth within two years of aspen harvesting (Verry et al., 1983). In a paired catchment experiment at the Marcell Experimental Forest (MEF) in north-central Minnesota, in a similar wetland-rich biophysical environment, water yield remained elevated in the 10 years after a forest harvest where ~70% of a small catchment was harvested, with the effect size decaying each year. However, in the 10th year after harvest, observed water yield was less than expected based on the pre-harvest calibration regression (Sebestyen et al., 2011), showing evidence that young forest in regional conditions can use more water than commercially mature forests. Finally, using catchment-aggregated USGS SSEBop remotely-sensed actual ET for 2000-2018 (Senay, 2018; Senay and Kagone, 2019), we found a significant (p<0.10, least-squares regression) positive correlation between AET and catchment-scale 11-year forest disturbance, indicating that catchments with more disturbance in the prior 11 years had higher AET. This is consistent with the streamflow decreases observed.

Hydrological recovery in this region is often considered ~15 years of regrowth based on research conducted at the MEF (Verry, 2004), and our recovery analysis found a similar time horizon at ~11 years, with decreased flows in the recovery period. Another related explanation for the decreased water yield associated with increased forest disturbance is the definition of "recovery" used. Our method of calculating recovery was based on whether a particular area with a forest disturbance was considered "disturbed" or not. Although conversion and regenerating disturbance was lumped, regenerating forest disturbance was often more important to the disturbance metric than conversion, especially when aggregated over the prior 11-13 years (Table 1). For the 11-year recovery window, forest harvested 1 year ago versus 10 years ago was considered as affecting water yield in the same way. If disturbed sites began

to use more water after the first few years following disturbance, then those years for which the young forest is using more water is lumped with those years in which it is using less into an aggregated metric. Supporting this, the general correlation of forest disturbance with streamflow is positive when recovery time is 1-3 years, but negative after that, for the St. Louis at Scanlon catchment. Thus, the 11 to 13-year disturbance recovery metric may be more aptly described as a "young forest" metric, grouping those portions of the catchment that have elevated ET post-disturbance. However, the Kawishiwi analysis found return to pre-disturbance streamflow after 5 years; it remains unclear what the effect could be >8 years after the fire, as effects were only estimated from 2012-2019.

Peak flows showed an inconsistent response to disturbance. The flood-frequency analysis for the Kawishiwi showed peak flows decreasing after the fire, but we were not confident in that effect; the regression analysis showed some increases and some decreases, but with no confidence >90%. For the St. Louis analysis, we were not confident in the effects of the forest disturbance on the Q2 peak flow in the flood-frequency framework, except for at the St. Louis near Forbes catchment, where we showed that increased forest disturbance was associated with decreased Q2 peak flows; this is consistent with the direction of effect in the Kawishiwi flood-frequency analysis, and with the water yield results. Reductions in peak flows have been found in the region due to desynchronization of snowmelt within a catchment, resulting in smaller peak flows after forest disturbance, which would be consistent with where reductions in peak flows were indicated in both frequency analyses (Verry et al., 1983; Sebestyen et al., 2011). For the St. Louis peak flow regression analysis, we were confident in some effects: two catchments showing a positive correlation between peak flows and forest disturbance, and two catchments showing a negative correlation with >90% confidence. In general, our findings are consistent with other studies that show the effect of forest disturbance on peak flows being more variable than the effect on water yield (Buttle, 2011).

Finally, only fast forest disturbances were considered in our analysis. There were several defoliation events associated with forest tent caterpillar in the St. Louis catchments within the study period (*Malacosoma disstria*; Cooke et al., 2022). However, defoliation due to tent caterpillar occurs in

the spring of the year when ET is generally energy-limited in the region, and affected trees re-foliate after invasion within the same year. Annually aggregated impacts of forest tent caterpillar on actual ET has been shown negligible in similar environments (Stephens et al., 2018). At the Scanlon gage where water yield data were available for the entire record, annual water yield climate-only model residuals were not well-correlated with tent caterpillar defoliation area (correlation = 0.06).

*4.2: Effect of Catchment Size*

The low relief of the landscape introduces some uncertainty into the analysis as well: the use of the 10m digital elevation model used by the version of StreamStats we used may not adequately have captured all basin boundaries. However, this effect is expected to be minor at these large scales, and because we did not conduct a strict "water balance" analysis where the tracking of accurate volumes is key, these delineation errors would likely just introduce additional variability accounted for in our regressions.

Our hypothesis that distinctive patterns associated with catchment spatial scale will be discernible in the catchment response to forest disturbance is supported: the lack of a strong effect of forest cover change on water yield and peak flows was due to climate variables comprising a majority of the runoff signal, and the small effects observed were likely attenuated by large-scale basin storage capacity in lakes and wetlands. This was illustrated in both the Kawishiwi and St. Louis catchments to varying degrees. In both catchments, a relative resiliency to forest disturbance was exhibited, as streamflow responses did not last long (<13 years in all instances, <5 years in the Kawishiwi), and total effects were small and difficult to observe with confidence. Most of the catchments in the St. Louis Basin did not have a confident correlation between water yield or peak flows and forest disturbance.

In the Kawishiwi catchment, in all 8 post-fire years, the climate variables accounted for 58% of the variability in post-fire water yield. Water yield increased at least 10mm above expected in only three post-fire years: years 2-4, and predicted streamflow variables were much more sensitive to climatic

variation. The lagged water yield response to the 2011 fire indicates a streamflow response strongly modulated by catchment storage dynamics (Table 3). Water yield did not significantly increase until year 2 after the fire (by 82 mm). The two driest years on record since streamgaging began in 1966 were 2010 and 2011 – the year before and the year of the fire. These dry conditions contributed to the large extent of the fire and the difficulty in extinguishing the Pagami Creek Fire (Kolka et al., 2014; Srock et al., 2018). Thus, there was likely a storage deficit that had to be replenished before the extra water in the catchment could be discharged as streamflow. In boreal Canadian Shield lake-dominated headwater catchments, lake storage deficit has been found to be a co-dominant driver of streamflow along with climate (Mielko and Woo, 2006; Spence, 2000), consistent with our findings where fire effects on streamflow show evidence of modulation by catchment storage demands.

In the St. Louis case study, even if there was a strongly correlated relationship between forest disturbance and peak flows, it could only account for up to ~20% of the variability in the Q2 through time. In fact, ~80% of the Q2 was explainable simply by basin spatial scale, and of the ~20% that was nonstationary, 49% was explained by winter*spring precipitation and only 2% by the 13-year forest disturbance. The mixed results of the peak flow regression, even where there was a >90% confidence correlation between forest disturbance and climate-detrended peak flows, had a much higher amount of variability explained by climate factors. The breakdown of stationary versus nonstationary components did not have a relationship with basin scale (Figure 5). However, the minimum basin scale was ~50 km$^2$, which is still two orders of magnitude larger than the experimental catchments at the Marcell Experimental Forest. Additionally, high confidence effects of forest disturbance on water yield in the St. Louis catchments decreased in magnitude with increasing basin size. There were only three catchments for which this condition applied, so it is unclear if this trend is generalizable. In general, streamflow in forested catchments with spatial area greater than 50 km$^2$ in low-relief glaciated regions is primarily influenced by climate variability and factors associated with basin spatial scale, while forest disturbance can have a detectable effect even at large catchment scales while being largely muted by fluctuations in climate drivers of streamflow. Overall, only marginal improvement (<10% variability explanation) is

granted by including forest disturbance as an explicit predictor of water yield and peak flows in the St. Louis case study.

## 5. Conclusion

We conclude that streamflow in large northern catchments is primarily controlled by climate drivers in the face of forest cover change at levels below the 30% areal disturbance analyzed in this study, but impacts can occur. Our work found that forest disturbance at low levels (<10%) within the prior 11-13 years can decrease water yield, possibly due to vigorous regrowth, but somewhere between 10-30% areal disturbance there is a shift where water yields increase following disturbance. Recovery time, or the time it takes for a regenerating forest to function hydrologically as it did before disturbance is likely ~5-13 years in the northern Lake States. This was illustrated in the Kawishiwi with a return to pre-fire water yields within 5 years, extending to a 13-year recovery for St. Louis basin peak flows. Effects of forest disturbance on the Q2 peak flows in the St. Louis basins are outweighed 4:1 by the effects of climate and basin size (Figure 5). In response to our hypotheses, we found that forest disturbance can both increase or decrease water yield depending on the disturbance regime, and equivocal evidence indicated that peak flows may increase or decrease, but peak flow results were less consistent and confident than water yield results. Where forest disturbance areas were small (approximately 1-10% of basin area) in the St. Louis catchments, < 10% of variability explanation was granted by including forest disturbance in models. However, consistent with a growing literature on the effects of partial forest disturbance in a catchment (e.g., Goeking & Tarboton, 2020; Bart et al., 2021, Segura et al., 2020), we found water yield *decreases* in response to higher forest disturbance levels under 10% of the basin area. Finally, our hypothesis that we would see clear signals of basin spatial scale within the streamflow response to forest disturbance was supported, in that the timing and relative size of climate versus forest disturbance effects pointed to the overall importance of climate variation and distributed catchment storage to streamflow generation.

## 6. Acknowledgements

## Works Cited

Ali, G, D. Tetzlaff, J.J. McDonnell, C. Soulsby, S. Carey, H. Laudon, K. McGuire, J. Buttle, J. Seibert, and J. Shanley. 2015. "Comparison of threshold hydrologic response across northern catchments." *Hydrological Processes* 29 (16): 3575-3591. doi:https://doi.org/10.1002/hyp.10527.

Alila, Y., Kuraś, P. K., Schnorbus, M., & Hudson, R. (2009). Forests and floods: A new paradigm sheds light on age-old controversies. *Water Resources Research*, *45*(8). https://doi.org/10.1029/2008wr007207

Andréassian, Vazken. 2004. "Waters and forests: from historical controversy to scientific debate." *Journal of Hydrology* 291 (1-2): 1-27. doi:https://doi.org/10.1016/j.jhydrol.2003.12.015.

Bart, R.R., R.L. Ray, M.H. Conklin, M. Safeeq, P.C. Saksa, C.L. Tague, and R.C. Bales. 2021. "Assessing the effects of forest biomass reductions on forest health and streamflow." *Hydrological Processes* 35 (3): e14114. doi:https://doi.org/10.1002/hyp.14114.

Bathurst, J.C., Fahey B, Iroumé A, and Jones J. 2020. "Forests and floods: using field evidence to reconcile analysis methods." *Hydrological Processes* 34 (15): 3295-3310. doi:https://doi.org/10.1002/hyp.13802.

Beguería S, Vicente-Serrano SM (2023). _SPEI: Calculation of the Standardized Precipitation-Evapotranspiration Index_. R package version 1.8.1, Available at https://CRAN.R-project.org/package=SPEI.

Bense, VF, T Gleeson, SE Loveless, O Bour, and J Scibek. 2013. "Fault zone hydrogeology." *Earth-Science Reviews* 127: 171-192. doi:https://doi.org/10.1016/j.earscirev.2013.09.008.

Blöschl, G. (2022). Three hypotheses on changing river flood hazards. *Hydrology and Earth System Sciences*, *26*(19), 5015-5033. https://doi.org/10.5194/hess-26-5015-2022

Blöschl, G., Ardoin-Bardin, S., Bonell, M., Dorninger, M., Goodrich, D., Gutknecht, D., Matamoros, D., Merz, B., Shand, P., & Szolgay, J. (2007). At what scales do climate variability and land cover change impact on flooding and low flows? *Hydrological Processes*, *21*(9), 1241-1247. https://doi.org/10.1002/hyp.6669

Bosch, J.M., and J.D. Hewlett. 1982. "A Review of Catchment Experiments to Determine the Effect of Vegetation Changes on Water Yield and Evapotranspiration." *Journal of Hydrology* 55: 3-23. doi:https://doi.org/10.1016/0022-1694(82)90117-2.

Brantley, S., C.R. Ford, and J.M. Vose. 2013. "Future species composition will affect forest water use after loss of eastern hemlock from southern Appalachian forests." *Ecological Applications* 23 (4): 777-790. doi:https://doi.org/10.1890/12-0616.1.

Brown, A.E., L. Zhang, T.A. McMahon, A.W. Western, and R.A. Vertessy. 2005. "A review of paired catchment studies for determining changes in water yield resulting from alterations in vegetation." *Journal of Hydrology* 310: 28-61. doi:https://doi.org/10.1016/j.jhydrol.2004.12.010.

Buttle, JM. 2011. "The effects of forest harvesting on forest hydrology and biogeochemistry." In *Forest Hydrology and Biogeochemistry*, edited by DF Levia, D Carlyle-Moses and T Tanaka, 659-677. Dordrecht: Springer.

Buttle, J. M., Beall, F. D., Webster, K. L., Hazlett, P. W., Creed, I. F., Semkin, R. G., & Jeffries, D. S. (2018). Hydrologic response to and recovery from differing silvicultural systems in a deciduous forest landscape with seasonal snow cover. *Journal of Hydrology*, *557*, 805-825. https://doi.org/10.1016/j.jhydrol.2018.01.006

Buttle, J. M., Webster, K. L., Hazlett, P. W., & Jeffries, D. S. (2019). Quickflow response to forest harvesting and recovery in a northern hardwood forest landscape. *Hydrological Processes*, *33*(1), 47-65. https://doi.org/10.1002/hyp.13310

Cooke, B.J., B.R. Sturtevant, and L.-E. Robert. 2022. "The Forest Tent Caterpillar in Minnesota: Detectability, Impact, and Cycling Dynamics." *Forests* 13: 601. doi:https://doi.org/10.3390/f13040601.

Dewitz, J, and U.S. Geological Survey. 2021. "National Land Cover Database (NLCD) 2019 Products (ver. 2.0, June 2021)." doi:10.5066/P9KZCM54.

Gelman, A., and D.B. Rubin. 1992. "Inference from Iterative Simulation Using Multiple Sequences." *Stat. Sci.* 7: 457-511.

Gelman, A., and F. Tuerlinckx. 2000. "Type S error rates classical and Bayesian single and multiple compparison procedures." *Comput. Stat.* 15: 373-390. doi:https://doi.org/10.1007/s001800000040.

Gelman, A., X. Meng, and H. Stern. 1996. "Posterior Predictive Assessment of Model Fitness via Realized Discrepancies." *Stat. Sin.* 6: 733-807.

Giles-Hansen, K., Li, Q., & Wei, X. (2019). The Cumulative Effects of Forest Disturbance and Climate Variability on Streamflow in the Deadman River Watershed. *Forests*, *10*(2). https://doi.org/10.3390/f10020196

Goeking, S.A., and D.G. Tarboton. 2020. "Forests and water yield: A synthesis of disturbance effects on streamflow and snowpack in western coniferous forests." *Journal of Forestry* 118 (2): 172-192. doi:https://doi.org/10.1093/jofore/fvz069.

Green, K. C., & Alila, Y. (2012). A paradigm shift in understanding and quantifying the effects of forest harvesting on floods in snow environments. *Water Resources Research*, *48*(10). https://doi.org/10.1029/2012wr012449

Guillemette, F., Plamondon, A. P., Prévost, M., & Lévesque, D. (2005). Rainfall generated stormflow response to clearcutting a boreal forest: peak flow comparison with 50 world-wide basin studies. *Journal of Hydrology*, *302*(1-4), 137-153. https://doi.org/10.1016/j.jhydrol.2004.06.043

Gumbel, EJ. 1958. *Statistics of Extremes*. New York: Columbia University Press.

Hewlett, J., Lull, H., & Reinhart, K. (1969). In Defense of Experimental Watersheds. *Water Resources Research*, *5*(1). https://doi.org/https://doi.org/10.1029/WR005i001p00306

Hewlett, J. D., & Hibbert, A. R. (1961). Increases in Water Yield after Several Types of Forest Cutting. *International Association of Scientific Hydrology. Bulletin*, *6*(3), 5-17. https://doi.org/10.1080/02626666109493224

Hobbs, H.C., and J.E. Goebel. 1982. "Geologic Map of Minnesota - Quaternary Geology. MGS Map S-1."

Homer, C.G., Dewitz, J.A., Yang, L., Jin, S., Danielson, P., Xian, G., Coulston, J., Herold, N.D., Wickham, J.D., Megown, K. 2015. "Completion of the 2011 National Land Cover Database for the coterminous United States-Representing a Decade of Land Cover Information." *Photogrammetric Engineering & Remote Sensing* 81 (5): 345-354.

Hou, Y., Wei, X., Vore, M., Déry, S. J., Pypker, T., & Giles-Hansen, K. (2022). Cumulative forest disturbances decrease runoff in two boreal forested watersheds of the northern interior of British Columbia, Canada. *Journal of Hydrology*, *605*. https://doi.org/10.1016/j.jhydrol.2021.127362

Ide, J. i., Finér, L., Laurén, A., Piirainen, S., & Launiainen, S. (2013). Effects of clear-cutting on annual and seasonal runoff from a boreal forest catchment in eastern Finland. *Forest Ecology and Management*, *304*, 482-491. https://doi.org/10.1016/j.foreco.2013.05.051

Iler, A. M., Inouye, D. W., Schmidt, N. M., & Hoye, T. T. (2017). Detrending phenological time series improves climate-phenology analyses and reveals evidence of plasticity. *Ecology*, *98*(3), 647-655. https://doi.org/10.1002/ecy.1690

Jirsa, M.A., T.J. Boerboom, V.W. Chandler, J.H. Mossler, A.C. Runkel, and D.R. Setterholm. 2011. "S-21 Geologic Map of Minnesota-Bedrock Geology."

Jones, J., & Grant, G. E. (1996). Peak Flow Responses to Clear-Cutting and Roads in Small and Large Basins, western Cascades, Oregon. *Water Resources Research*, *32*(4), 959-974. https://doi.org/https://doi.org/10.1029/95WR03493

Kass, R.E., and A. Rafferty. 1995. "Bayes ratios." *Journal of American Statistical Association* 90: 773-795.

Kennedy, R.E., Yang, Z. and Cohen, W.B., 2010. Detecting trends in forest disturbance and recovery using yearly Landsat time series: 1. LandTrendr—Temporal segmentation algorithms. *Remote Sensing of Environment*, *114*(12), pp.2897-2910.

Kolka, R., B. Sturtevant, P. Townsend, J. Miesel, P. Wolter, S. Fraver, and T. DeSutter. 2014. "Post-Fire Comparisons of Forest Floor and Soil Carbon, Nitrogen, and Mercury Pools with Fire Severity Indices." *Soil Sci. Soc. Am. J. North Am. For. Soils Conf. Proc. 78* S58-S65. doi:https://doi.org/10.2136/sssaj2013.08.0351nafsc.

Laudon, H. and Sponseller, R.A., 2018. How landscape organization and scale shape catchment hydrology and biogeochemistry: Insights from a long-term catchment study. *Wiley Interdisciplinary Reviews: Water*, *5*(2), p.e1265.

Likens, Gene E. 2001. "Biogeochemistry, the watershed approach: some uses and limitations." *Marine and Freshwater Research* 52 (1): 5-12. doi:https://doi.org/10.1071/MF99188.

Lima, C.H., and U. Lall. 2010. "Spatial scaling in a changing climate: A hierarchical bayesian model for non-stationary multi-site annual maximum and monthly streamflow." *Journal of Hydrology* 383 (3-4): 307-318. doi:https://doi.org/10.1016/j.jhydrol.2009.12.045.

Lin, Y., & Wei, X. (2008). The impact of large-scale forest harvesting on hydrology in the Willow watershed of Central British Columbia. *Journal of Hydrology*, *359*(1-2), 141-149. https://doi.org/10.1016/j.jhydrol.2008.06.023

Loftis, J. C, L. H. MacDonald, S. Streett, H.K. Iyer, and K. Bunte. 2001. "Detecting cumulative watershed effects: the statistical power of pairing." *Journal of Hydrology* 251 (1-2): 49-64. doi:https://doi.org/10.1016/S0022-1694(01)00431-0.

McEachran, Z.P., D.L. Karwan, S.D. Sebestyen, R.A. Slesak, and G.H.C. Ng. 2021. "Nonstationary flood-frequency analysis to assess effects of harvest and cover type conversion on peak flows at the Marcell Experimental Forest, Minnesota, USA." *Journal of Hydrology* 596: 126054. doi:https://doi.org/10.1016/j.jhydrol.2021.126054.

McEachran, Z. P., Karwan, D. L., & Slesak, R. A. (2020). Direct and Indirect Effects of Forest Harvesting on Sediment Yield in Forested Watersheds of the United States. *JAWRA Journal of the American Water Resources Association*, *57*(1), 1-31. https://doi.org/10.1111/1752-1688.12895

McShane, B.B., D. Gal, A. Gelman, C. Robert, and J.L. Tackett. 2019. "Abandon Statistical Significance." *Am. Stat.* 73: 235-245. doi:https://doi.org/10.1080/00031305.2018.1527253.

Mengistu, S.G., I.F. Creed, R.J. Kulperger, and C.G. Quick. 2013. "Russian nesting dolls effect – Using wavelet analysis to reveal non-stationary and nested stationary signals in water yield from catchments on a northern forested landscape." *Hydrological Processes* 27: 669-686. doi:https://doi.org/10.1002/hyp.9552.

Menne, M.J., I. Durre, B. Korzeniewski, S. McNeal, K. Thomas, X. Yin, S. Anthony, et al. 2012. *Global Historical Climatology Network - Daily (GHCN-Daily), Version 3.26.* NOAA National Climatic Data Center. Accessed December 2019. doi:http://doi.org/10.7289/V5D21VHZ.

Menne, M.J., I. Durre, R.S. Vose, B.E. Gleason, and T.G. Houston. 2012. "An overview of the global historical climatology network-daily database." *J. Atmos. Ocean. Technol.* 29: 897-910. doi:https://doi.org/10.1175/JTECH-D-11-00103.1.

Mielko, C., and M.K. Woo. 2006. "Snowmelt runoff processes in a headwater lake and its catchment, subarctic Canadian Shield." *Hydrological Processes* 20: 987-1000. doi:https://doi.org/10.1002/hyp.6117.

Minnesota Department of Natural Resources. 2022. "Minnesota DNR Hydrography Dataset." Accessed 10 4, 2022. https://resources.gisdata.mn.gov/pub/gdrs/data/pub/us_mn_state_dnr/water_dnr_hydrography/metadata/metadata.html.

Minnesota National Wetlands Inventory. 2019. Accessed 06 18, 2019. https://gisdata.mn.gov/dataset/water-nat-wetlands-inv-2009-2014.

Neary, D. (2016). Long-Term Forest Paired Catchment Studies: What Do They Tell Us That Landscape-Level Monitoring Does Not? *Forests*, *7*(12). https://doi.org/10.3390/f7080164

NOAA-NCEI. 2020. "Weather Data for Winton Power Plant, Station #USC00219101, Period of Record 1966-1995." Accessed 12 2019. https://www.ncdc.noaa.gov/cdo-web/datasets.

National Oceanic and Atmospheric Administration – Physical Sciences Laboratory (NOAA-PSL) (2020). Atlantic Multidecadal Oscillation, Pacific Decadal Oscillation, North Atlantic Oscillation, and Multivariate El Niño Southern Oscillation (ENSO) Index (MEI) data. AMO data accessed from https://psl.noaa.gov/data/timeseries/AMO/ on 07/07/2020.

Phillips, C.B., and D.J. Jerolmack. 2016. "Self-organization of river channels as a critical filter on climate signals." *Science* 352: 694-698. doi:https://doi.org/10.1126/science.aad3348.

Pierson, F.B., J.D. Bates, T.C Svejcar, and S.P. Hardegree. 2007. "Runoff and erosion after cutting western Juniper." *Rangeland Ecology and Management* 60 (3): 285-292. doi:https://doi.org/10.2111/1551-5028(2007)60[285:RAEACW]2.0.CO;2.

Plummer, M. 2003. "JAGS: A program for analysis of Bayesian graphical models using Gibbs sampling." *Proc. 3rd Int. Work. Distrib. Stat. Comput. (DSC 2003)* 20-22. doi:https://doi.org/10.1.1.13.3406.

Prettyman, D.H. 1978. "Soil Survey of Kawishiwi Area, Minnesota: Parts of Lake and Cook Counties in Superior National Forest."

PRISM Climate Group. 2020. *http://prism.oregonstate.edu, created 4 Feb 2004. Update: 07/15/2020. Accessed 07/18/2020.* Oregon State University.

R Core Team. 2022. "R: A language and environment for statistical computing."

Rogger, M., M. Agnoletti, A. Alaoui, J. C. Bathurst, G. Bodner, M. Borga, V. Chaplot, et al. 2017. "Land use change impacts on floods at the catchment scale: Challenges and opportunities for future research." *Water Resources Research* 53 (7): 5209-5219. doi:https://doi.org/10.1002/2017WR020723.

Safeeq, M., Grant, G. E., Lewis, S. L., & Hayes, S. K. (2020). Disentangling effects of forest harvest on long-term hydrologic and sediment dynamics, western Cascades, Oregon. *Journal of Hydrology*, *580*. https://doi.org/10.1016/j.jhydrol.2019.124259

Sahin, V., & Hall, M. J. (1996). The effects of afforestation and deforestation on water yields. *Journal of Hydrology*, *178*(1-4), 293-309. https://doi.org/https://doi.org/10.1016/0022-1694(95)02825-0

Sebestyen, SA, ES Verry, and KN Brooks. 2011. "Hydrological Responses to Changes in Forest Cover on Uplands and Peatlands." In *Peatland Biogeochemistry and Watershed Hydrology at the Marcell Experimental Forest*, edited by RK Kolka, SD Sebestyen, ES Verry and KN Brooks, 401-432. Boca Raton, FL: CRC Press.

Segura, C., Bladon, K. D., Hatten, J. A., Jones, J. A., Hale, V. C., & Ice, G. G. (2020). Long-term effects of forest harvesting on summer low flow deficits in the Coast Range of Oregon. *Journal of Hydrology*, *585*. https://doi.org/10.1016/j.jhydrol.2020.124749

Senay, G. 2018. "Satellite Psychrometric Formulation of the Operational Simplified Surface Energy Balance (SSEBop) Model for Quantifying and Mapping Evapotranspiration." *Applied Engineering in Agriculture* 34 (3): 555-566. doi:https://doi.org/10.13031/aea.12614 .

Senay, G.B., and S. Kagone. 2019. *Daily SSEBop Evapotranspiration: U. S. Geological Survey Data Release.* US Geological Survey. doi:https://doi.org/10.5066/P9L2YMV.

Spence, C. 2000. "The Effect of Storage on Runoff from a Headwater Subarctic Shield Basin." *Arctic* 53: 237-247.

Srock, A.F., J.J. Charney, B.E. Potter, and S.L. Goodrick. 2018. "The Hot-Dry-Windy Index : A New Fire Weather Index." *Atmosphere* 9 (11). doi:https://doi.org/10.3390/atmos9070279.

Stednick, JD. 1996. "Monitoring the effects of timber harvest on annual water yield." *Journal of Hydrology* 176: 79-95. doi:https://doi.org/10.1016/0022-1694(95)02780-7.

Stephens JJ, Black TA, Jassal RS, Nesic Z, Grant NJ, Barr AG, Helgason WD, Richardson AD, Johnson MS, and Christen A. 2018. "Effects of forest tent caterpillar defoliation on carbon and water fluxes in a boreal aspen stand." *Agricultural and Forest Meteorology* 253-254: 176-189. doi:https://doi.org/10.1016/j.agrformet.2018.01.035.

Su, Y.-S., and M. Yajima. 2015. "R2jags: Using R to Run "JAGS"."

Thomas, R. B., & Megahan, W. F. (1998). Peak flow responses to clear-cutting and roads in small and large basins, Western Cascades, Oregon: A second opinion. *Water Resources Research*, *34*(12), 3393-3403. https://doi.org/10.1029/98wr02500

U.S. Geological Survey. 2016. "The StreamStats program, Version 4." Accessed 9 2018. http://streamstats.usgs.gov.

Verry, E.S. 2004. "Land Fragmentation and Impacts to Streams and Fish in the Central and Upper Midwest." In *A Century of Forest and Wildland Watershed Lessons*, edited by G.G. Ice and J.D. Stednick, 129-154. Bethesda, MD: Society of American Foresters.

Verry, E.S., J.R. Lewis, and K.N. Brooks. 1983. "Aspen Clearcutting increases Snowmelt and Storm Flow Peaks in North Central Minnesota." *Water Resources Bulletin* 19: 59-67.

Viglione, A., Merz, B., Viet Dung, N., Parajka, J., Nester, T. and Blöschl, G., 2016. Attribution of regional flood changes based on scaling fingerprints. *Water resources research*, *52*(7), pp.5322-5340.

Vogeler, J.C., 2019. "Most recent fast forest disturbances in Minnesota, Version 3.0." Accessed 2019. https://resources.gisdata.mn.gov/pub/gdrs/data/pub/us_mn_state_dnr/env_fast_forest_disturbances/metadata/metadata.html.

Vogeler, J.C., R.A. Slesak, P.A. Fekety, and M.J. Falkowski. 2020. "Characterizing over Four Decades of Forest Disturbance in Minnesota , USA." *Forests* 11: 1-18. doi:https://doi.org/10.3390/f11030362.

Wei, X., Hou, Y., Zhang, M., Li, Q., Giles-Hansen, K., & Liu, W. (2021). R eexamining forest disturbance thresholds for managing cumulative hydrological impacts. *Ecohydrology*, *14*(8). https://doi.org/10.1002/eco.2347

Wolman, MG, and JP Miller. 1960. "Magnitude and Frequency of Forces in Geomorphic Processes." *Journal of Geology* 68: 54-74.

Zégre, Nicolas, Arne N. Skaugset, Nicholas A. Som, Jeffery J. McDonnell, and Lisa M. Ganio. 2010. "In lieu of the paired catchment approach: Hydrologic model change detection at the catchment scale." *Water Resources Research* 46 (11). doi:https://doi.org/10.1029/2009WR008601.

Zhang, M, Liu N, Harper R, Li Q, Liu K, Wei X, Ning D, Hou Y, and Liu S. 2017. "A global review on hydrological responses to forest change across multiple spatial scales: Importance of scale, climate, forest type and hydrological regime." *Journal of Hydrology* 546: 44-59. doi:https://doi.org/10.1016/j.jhydrol.2016.12.040.

*Table 1: Catchment characteristics for the St. Louis Basin catchments. Note that some basins had an extra 1-2 years of data for annual maximum flow due to records being available during spring freshet, while water yield record periods are reported in the table.*

| Catchment | Size [Km²] | Years Streamflow Record | Upland Forest [% catchment area] | Woody Wetlands [% catchment area] | Herbaceous Wetlands + Open Water [% catchment area] | Average Annual Regenerating Forest Disturbance [% catchment area] | Cumulative Conversion since 1986 [% catchment area] |
|---|---|---|---|---|---|---|---|
| Second Creek near Aurora | 56 | 2009-2018 | 34 | 22 | 19 | 0.27 | 1.3 |
| Colvin Creek near Hoyt Lakes | 58 | 2015-2018 | 38 | 52 | 7 | 0.43 | 0.02 |
| Stoney Brook near Brookston | 192 | 2007-2018 | 23 | 63 | 10 | 0.32 | 0.31 |
| Partridge River at Hoyt Lakes | 270 | 1986-1988; 2002 | 37 | 52 | 5 | 0.40 | 0.03 |
| Partridge River near Hoyt Lakes | 333 | 2010-2018 | 37 | 48 | 7 | 0.40 | 0.21 |
| Swan River near Toivola | 620 | 2011-2018 | 32 | 43 | 7 | 0.26 | 1.2 |
| St Louis River near Aurora | 756 | 1986-1987; 2014-2015 | 32 | 53 | 8 | 0.36 | 0.27 |
| Whiteface River near Meadowlands | 1354 | 2012-2018 | 26 | 62 | 7 | 0.41 | 0.15 |
| St Louis River near Forbes | 1791 | 1986-1989; 2010-2018 | 34 | 49 | 7 | 0.38 | 0.49 |
| Cloquet River near Burnett | 2028 | 2009-2017 | 39 | 46 | 7 | 0.48 | 0.37 |
| St Louis River at Scanlon | 8884 | 1986-2018 | 30 | 53 | 7 | 0.35 | 0.45 |

*Table 2: Data used in the analysis of annual water yield and annual maximum peak daily streamflow.*

| Annual Water Yield | Basins Used | Equation 5 Key | Data Citation | Annual Maximum Daily Streamflow | Basins Used | Data Source |
|---|---|---|---|---|---|---|
| Annual precipitation* | K, STL | *P* | PRISM Climate Group, 2020 | Winter precipitation | K, STL | PRISM Climate Group, 2020 |
| Previous year's runoff ratio (to | K | | USGS, 2016; PRISM Climate Group, 2020 | Spring precipitation | K, STL | PRISM Climate Group, 2020 |

| | | | | | | |
|---|---|---|---|---|---|---|
| capture antecedent wetness) | | | | | | |
| September-October Precipitation (for antecedent wetness) | STL | | PRISM Climate Group, 2020 | September-October Precipitation (for antecedent wetness) | STL | PRISM Climate Group, 2020 |
| Annual average monthly temperature* | K, STL | | PRISM Climate Group, 2020 | Average monthly winter temperature | K, STL | PRISM Climate Group, 2020 |
| Annual average monthly dew point temperature* | K, STL | | PRISM Climate Group, 2020 | | | |
| Annual average minimum monthly vapor pressure deficit* | K, STL | | PRISM Climate Group, 2020 | | | |
| Annual average maximum monthly vapor pressure deficit* | K, STL | VPD | PRISM Climate Group, 2020 | | | |
| First principal component of: monthly maximum, minimum vapor pressure deficit, monthly mean air and dewpoint temperatures, and annual total Thornthwaite PET. Explained 62.6% of the total variance in those terms. | STL | ET.PCA1 | PRISM Climate Group, 2020; SPEI Package in R | | | |
| Thornthwaite PET | K, STL | PET | PRISM Climate Group, 2020 SPEI package in R (Beguería & Vicente-Serrano, 2023) | | | |

*Table 3: Water yield on the Upper Kawishiwi catchment after the Pagami Creek Fire, N years after the fire. Years with > 90% confidence in water yield increases are marked with \*. Expected water yield was that based on the pre-fire model. Confidence that the water yield decreased equals one minus the confidence that water yield increased.*

| Years after the fire | 1 | 2 | 3 | 4 | 5 | 6 | 7 | 8 |
|---|---|---|---|---|---|---|---|---|
| Expected (sd) [mm] | 263 (58) | 274 (58) | 312 (59) | 175 (59) | 309 (64) | 346 (66) | 256 (56) | 295 (58) |
| Observed [mm] | 212 | 356 | 367 | 210 | 312 | 351 | 251 | 286 |
| Confidence that Water Yield Increased | 19% | 92% * | 83% | 73% | 52% | 54% | 46% | 44% |

*Table 4: ANCOVA-based annual maximum flows on the Upper Kawishiwi catchment after the Pagami Creek Fire. Expected peak flow was that based on the pre-fire model. Confidence that the peak flow decreased equals one minus the confidence that peak flow increased.*

| Years after the fire | 1 | 2 | 3 | 4 | 5 | 6 | 7 | 8 |
|---|---|---|---|---|---|---|---|---|
| Expected (sd) [mm/day] | 2.88 (1.16) | 3.27 (1.16) | 3.57 (1.19) | 2.36 (1.19) | 4.76 (1.39) | 3.87 (1.33) | 2.11 (1.17) | 3.69 (1.17) |
| Observed [mm/day] | 2.90 | 3.56 | 4.97 | 2.25 | 3.31 | 3.35 | 2.01 | 3.16 |
| Confidence that Peak Flow Increased | 51% | 60% | 88% | 47% | 14% | 35% | 46% | 32% |

*Table 5: Water Yield effect parameter for the St. Louis catchments LME-residuals model. Where our confidence that the water yield decreased is greater than 90%, we marked with * .*

| Catchment | Effect Parameter $b_r$ [mm of water yield change from expected, per additional percentage of forest disturbed in last 11 years or permanently converted] | P($b_r$ < 0) [%] |
|---|---|---|
| Second Creek near Aurora | -19 [-25 to -12] | 100% * |
| Colvin Creek near Hoyt Lakes | 2 [-20 to 22] | 44% |
| Stoney Brook near Brookston | -4 [-31 to 22] | 59% |
| Partridge River at Hoyt Lakes | 3 [-6 to 12] | 28% |
| Partridge River near Hoyt Lakes | -2 [-13 to 10] | 59% |
| Swan River near Toivola | -9 [-34 to 17] | 73% |
| St Louis River near Aurora | 3 [-7 to 12] | 33% |
| Whiteface River near Meadowlands | 4 [-17 to 24] | 38% |
| St Louis River near Forbes | -13 [-18 to -8] | 100% * |
| Cloquet River near Burnett | 1 [-17 to 20] | 45% |
| St Louis River at Scanlon | -9 [-13 to -5] | 100% * |

*Table 6: Peak Flow effects for the St. Louis catchments LME-residuals model. Where confidence in peak flow decreases, or increases, were >90%, we marked with a * .*

| Catchment | Effect Parameter $b_r$ [m³/s / 100km² peak flow change from expected, per additional percentage of forest disturbed in last 11 years or permanently converted] | P($b_r$ < 0) [%] |
|---|---|---|
| Second Creek near Aurora | -0.3 [-0.7 to 0.05] | 92% * |
| Colvin Creek near Hoyt Lakes | 0.4 [-1.9 to 2.7] | 38% |
| Stoney Brook near Brookston | 3.3 [1.7 to 4.9] | <1% (>99% confidence $b_r$ > 0) * |
| Partridge River at Hoyt Lakes | 0.3 [-0.1 to 0.6] | 13% |
| Partridge River near Hoyt Lakes | -0.3 [-1.2 to 0.6] | 73% |
| Swan River near Toivola | -1.4 [-3.5 to 0.7] | 86% |
| St Louis River near Aurora | -0.4 [-0.7 to -0.08] | 98% * |
| Whiteface River near Meadowlands | 1.9 [1.0 to 2.8] | < 1% (>99% confidence $b_r$ > 0)* |
| St Louis River near Forbes | -0.2 [-0.4 to -0.01] | 96% * |
| Cloquet River near Burnett | 7.2 [2.0 to 12.2] | 1% (99% confidence $b_r$ > 0) * |

*Table 7: Forest disturbance and winter\*spring precipitation effects parameters, for the probabilistic model of Q2 streamflow on the St. Louis Basin. \* indicate high-confidence effects parameters where confidence in the effect being greater than or less than zero is >90%.*

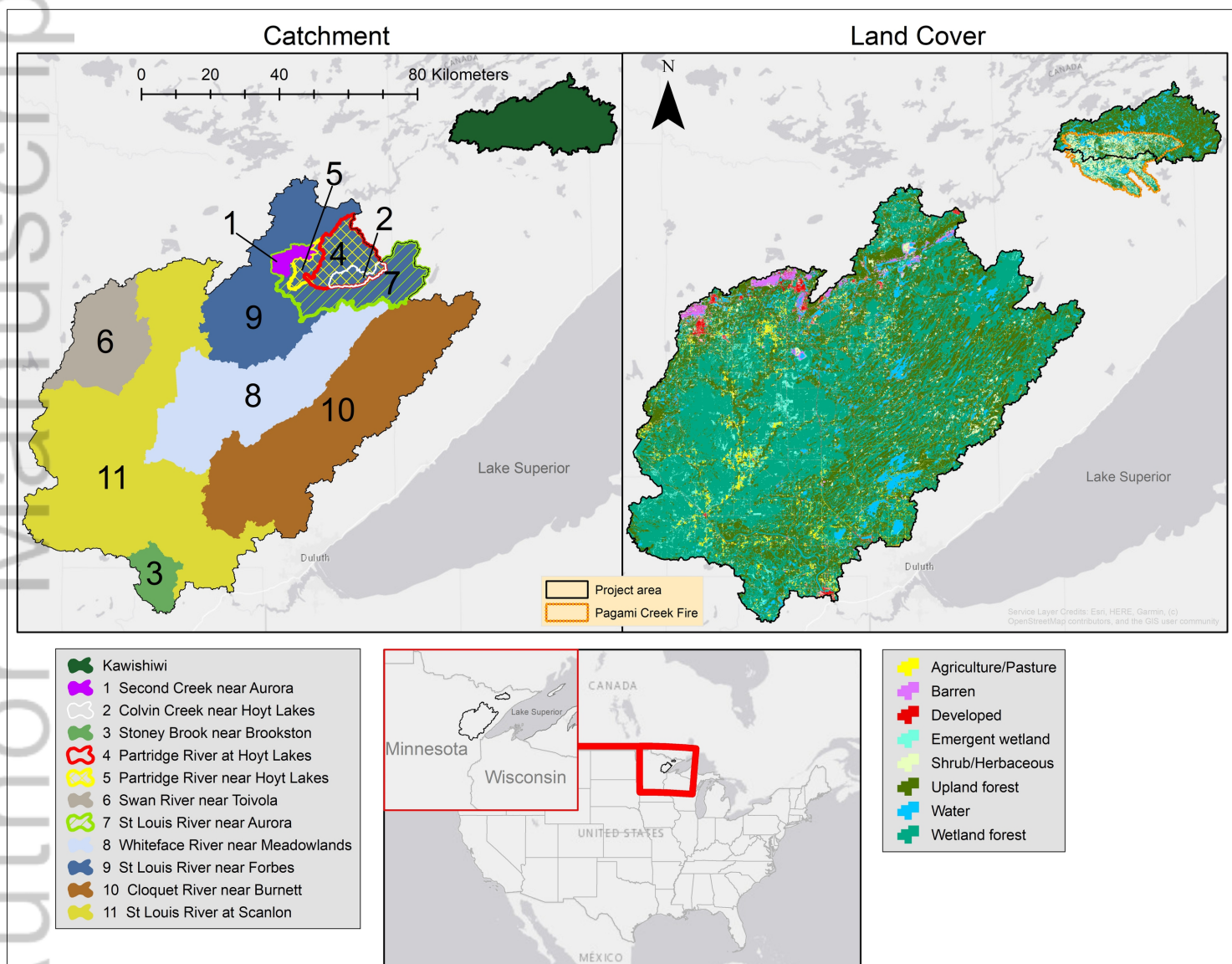| Catchment | Forest disturbance effect parameter [m³/s per additional percentage forest disturbance] | Precipitation effect parameter [m³/s per standard deviation of winter times spring precipitation] |
|---|---|---|
| Second Creek near Aurora | -0.13 (-0.33 to 0.08) | 0.19 (-0.25 to 0.67) |
| Colvin Creek near Hoyt Lakes | -0.37 (-1.1 to 0.38) | -0.01 (-4.1 to 4.6) |
| Stoney Brook near Brookston | 1.7 (-0.71 to 3.9) | 2.5 (1.2 to 3.8) * |
| Partridge River at Hoyt Lakes | -0.29 (-9.4 to 8.1) | 3.0 (-29 to 39) |
| Partridge River near Hoyt Lakes | -0.09 (-2.4 to 1.9) | 3.4 (1.4 to 5.5) * |
| Swan River near Toivola | -4.3 (-12 to 3.2) | 7.5 (0.56 to 14.4) * |
| St Louis River near Aurora | -1.5 (-5.4 to 1.8) | 2.6 (-6.0 to 12) |
| Whiteface River near Meadowlands | -0.91 (-17 to 14) | 11.1 (-22 to 47) |
| St Louis River near Forbes | -2.3 (-4.3 to -0.37) * | 13.3 (7.6 to 19) * |
| Cloquet River near Burnett | -10.7 (-27.7 to 5.8) | 23 (-31 to 80) |
| St Louis River at Scanlon | -9.0 (-21 to 3.0) | 92 (59 to 125) * |

Figure1_new.jpg
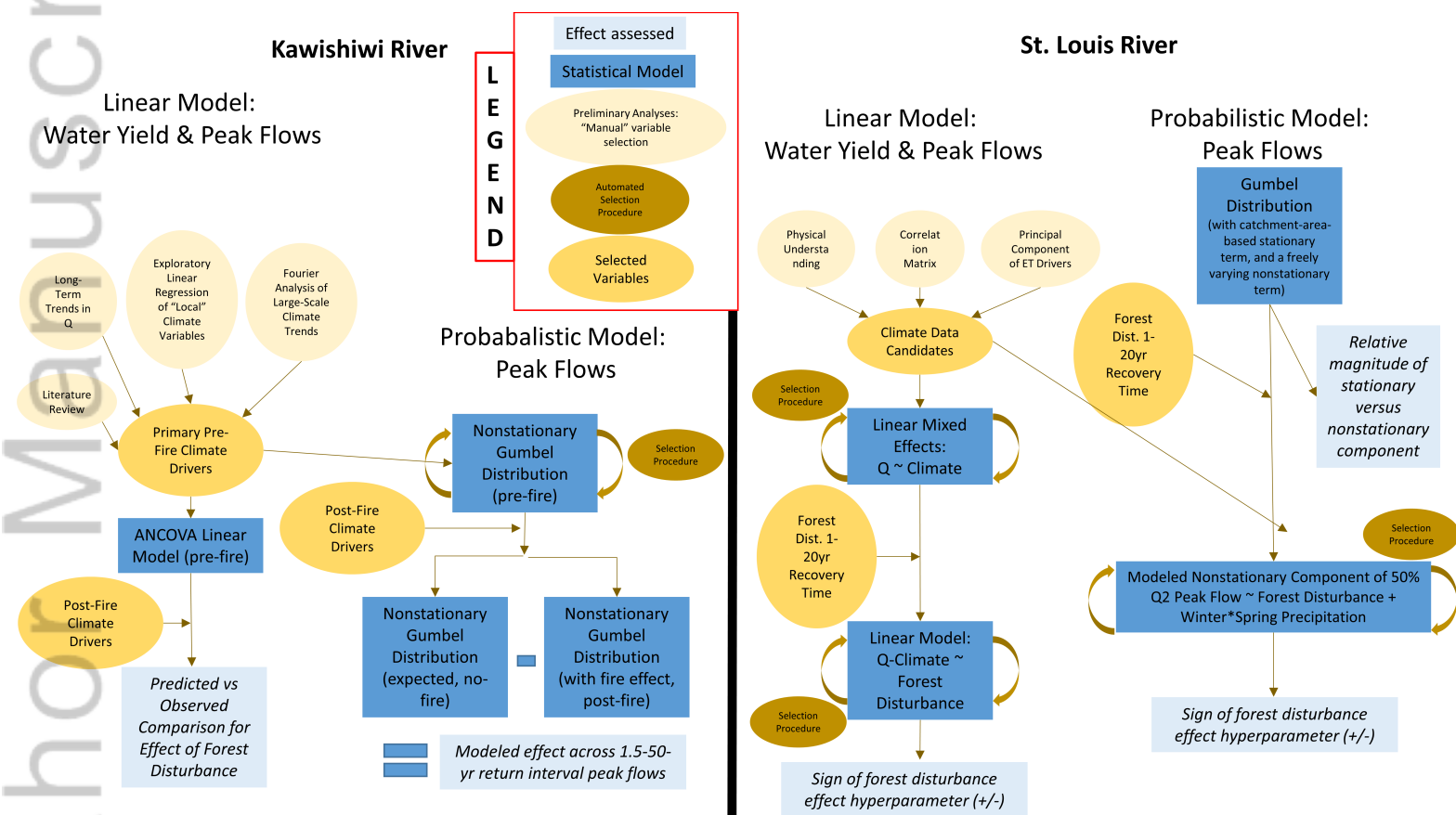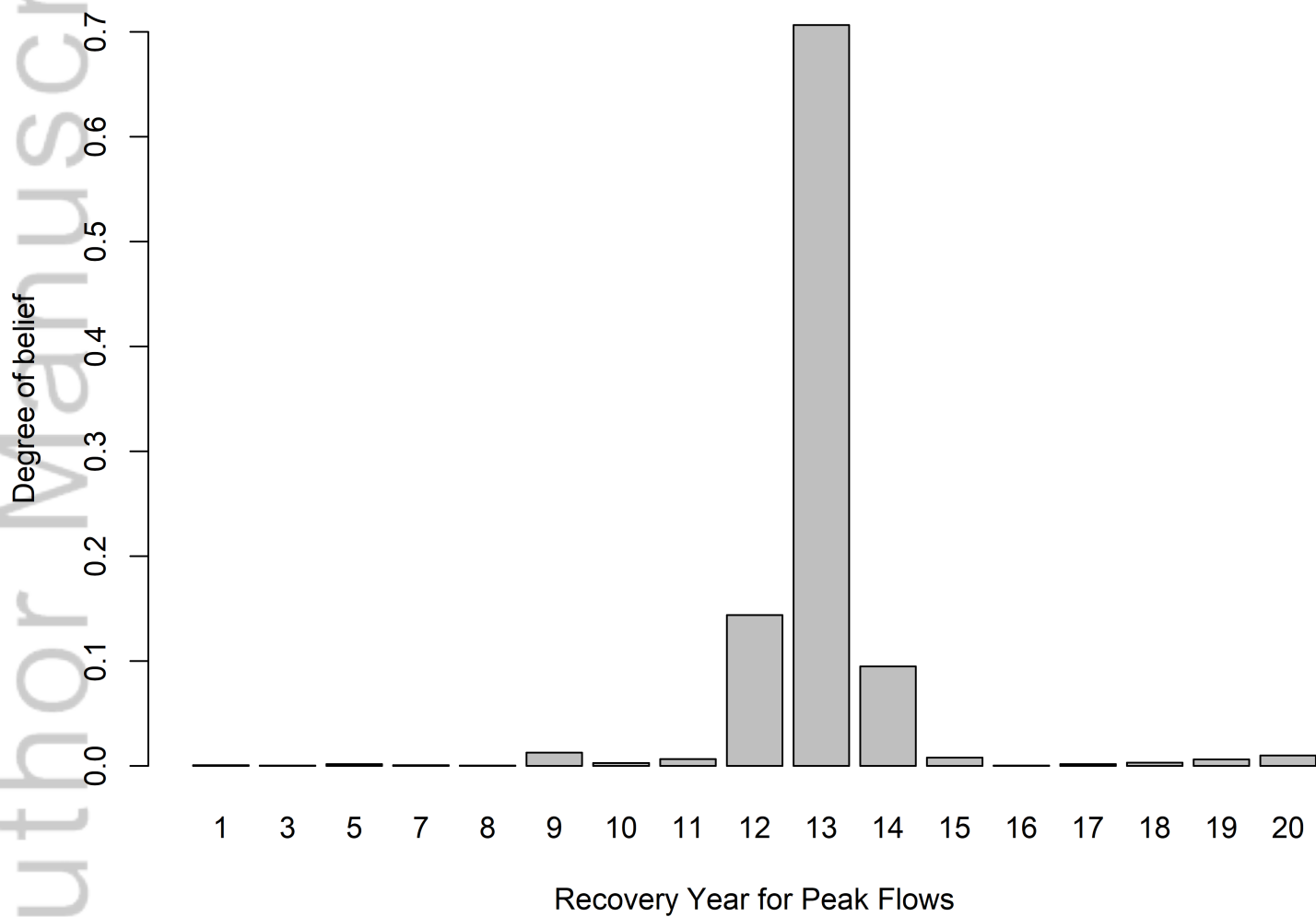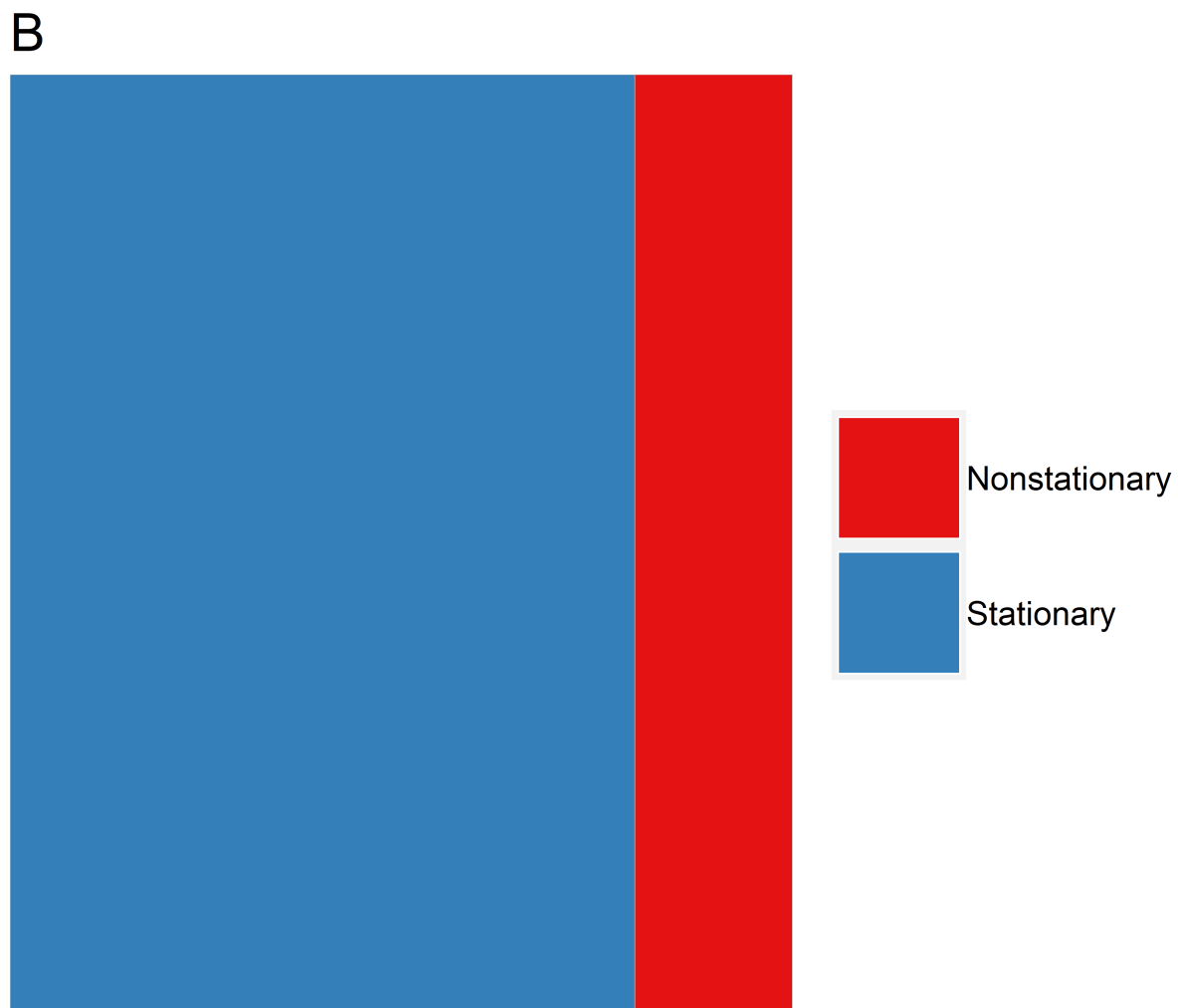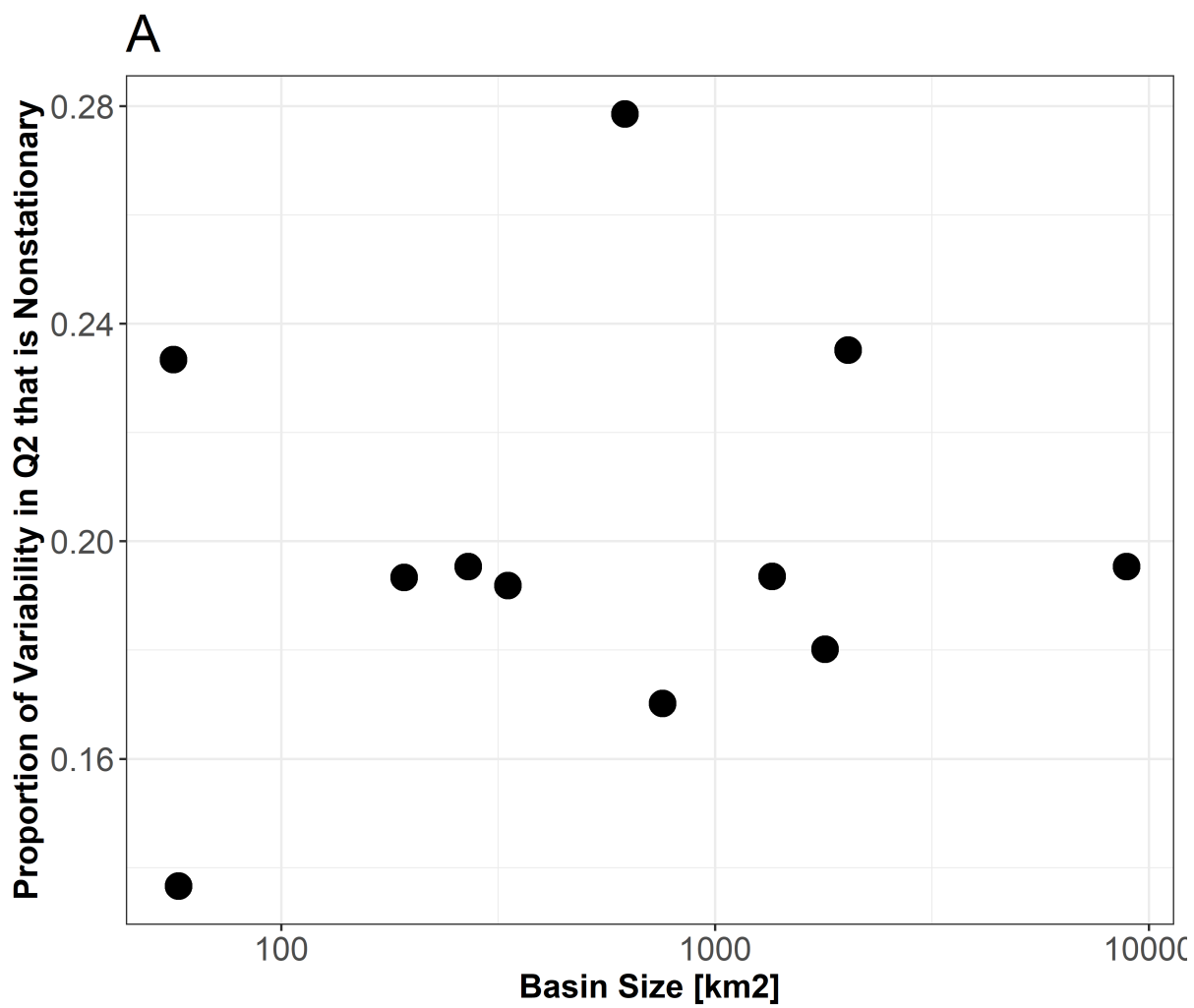
Figure2.png
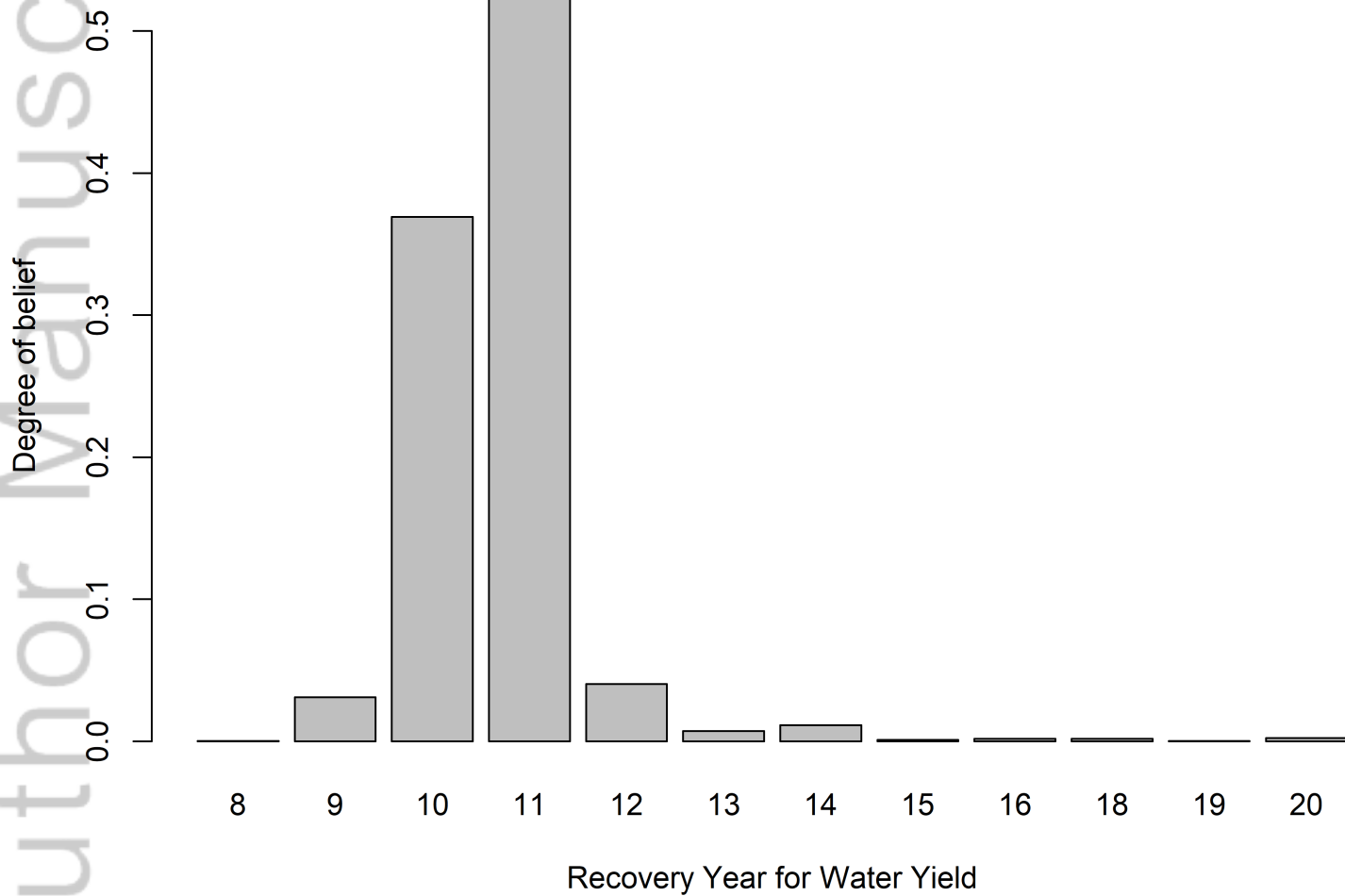
Figure3.png

Figure4.png

A



B



Figure5.png

Figure 1: Basins and geographic setting.

Figure 2: Workflow diagram for the analysis techniques used to assess effects of forest disturbance on streamflow on the Kawishiwi and St. Louis River

Figure 3: Hydrologic recovery year for water yield after forest disturbance, after adjusting for the effects of climate. The Degree-of-Belief represents how confident we are that the N year recovery year is the best-fitting model for recovery years 1-20. Recovery year represents the number of years after a forest disturbance such as fire, harvest, or windthrow when that parcel no longer influences the water yield regression as a "disturbed" parcel, and was selected according to best-fit of the regression.

Figure 4: Hydrologic recovery year for peak flow after forest disturbance, after adjusting for the effects of climate. The Degree-of-Belief represents how confident we are that the N year recovery year is the best-fitting model for recovery years 1-20. Recovery year represents the number of years after a forest disturbance such as fire, harvest, or windthrow when that parcel no longer influences the peak flow regression as a "disturbed" parcel, and was selected according to best-fit of the regression.

Figure 5: a) Nonstationary component of the Q2, or 50% exceedance probability annual maximum streamflow, that can vary year-to-year, as a proportion of the overall magnitude of the Q2 across all years, for each catchment; b) overall average across catchments, across years, variability in the Q2 attributable to stationary versus nonstationary processes.

**Annual Maximum Streamflow: 50% Exceedence Probability**

Stationary Process

Nonstationary Process
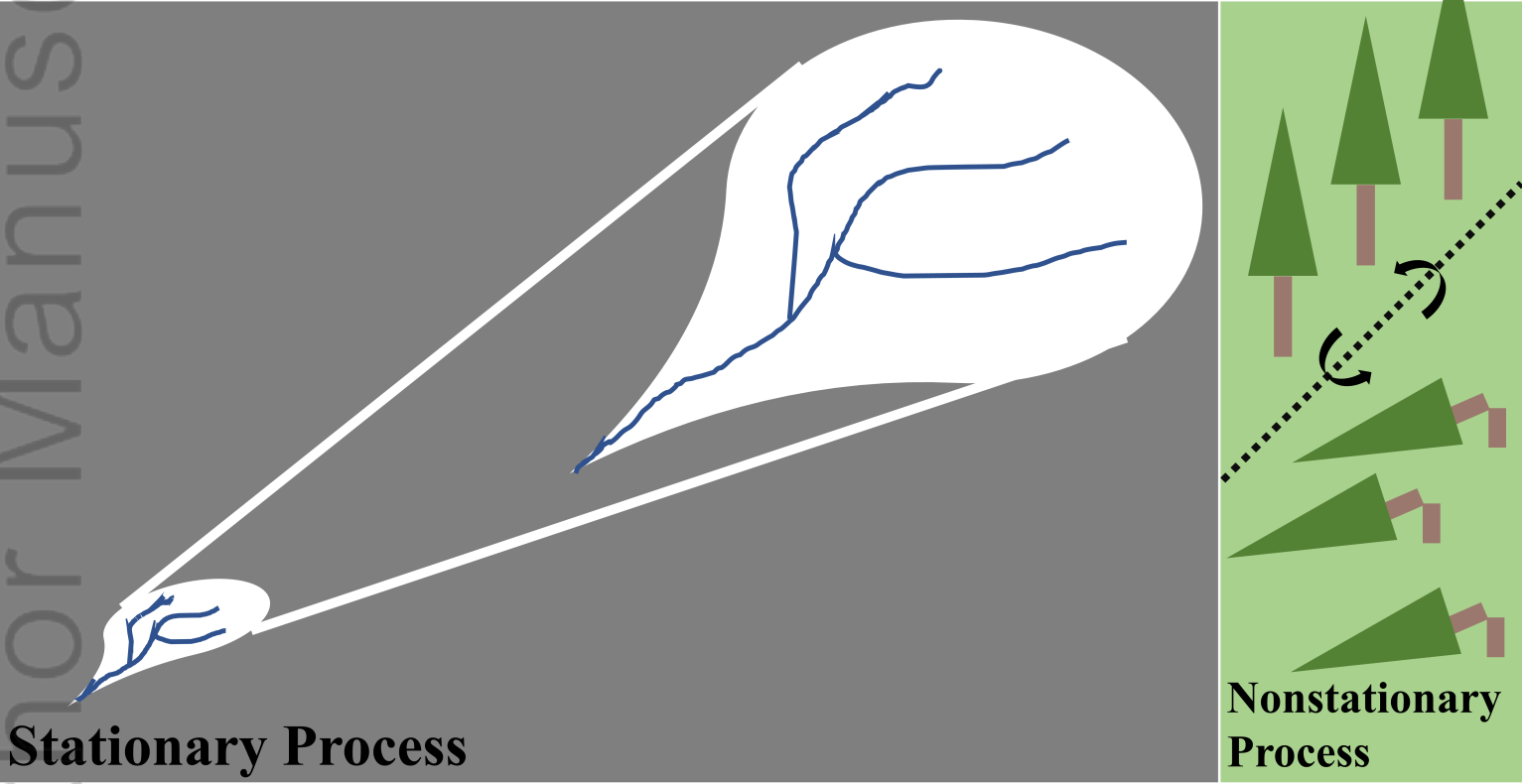
GraphicalAbstract.png

**Effects of forest disturbance on water yield and peak flow in low-relief glaciated catchments assessed with Bayesian parameter estimation**

McEachran, Zachary P.[1*], Reese, Gordon[2]; Karwan, Diana L.[3]; Slesak, Robert A.[4]; Vogeler, Jody[5]

[1] NOAA National Weather Service North Central River Forecast Center, Chanhassen, MN 55317

[2] USDA Forest Service, Northern Research Station, Rhinelander, WI, USA 54501

[3] University of Minnesota, Department of Forest Resources, St. Paul, MN 55108

[4] USDA Forest Service, Pacific Northwest Research Station, Olympia WA 98512

[5] Natural Resources Ecology Laboratory, Colorado State University, Fort Collins CO 80526

\* [zachary.mceachran@noaa.gov](mailto:zachary.mceachran@noaa.gov)

**Graphical Abstract Text:**

The catchment approach has been traditionally limited to small catchments; however, larger catchments may have emergent streamflow drivers. We used statistical models of water yield and peak streamflow for forested catchments in Minnesota to investigate forest disturbance effects on streamflow at large scales. Streamflow was resilient to forest cover change, but we did observe some impacts. Stationary basin-scale signals were the primary drivers of streamflow, explaining ~80% of the magnitude of the 50% annual exceedance probability peak flow.

*Table 1: Catchment characteristics for the St. Louis Basin catchments. Note that some basins had an extra 1-2 years of data for annual maximum flow due to records being available during spring freshet, while water yield record periods are reported in the table.*

| Catchment | Size [Km²] | Years Streamflow Record | Upland Forest [% catchment area] | Woody Wetlands [% catchment area] | Herbaceous Wetlands + Open Water [% catchment area] | Average Annual Regenerating Forest Disturbance [% catchment area] | Cumulative Conversion since 1986 [% catchment area] |
|---|---|---|---|---|---|---|---|
| Second Creek near Aurora | 56 | 2009-2018 | 34 | 22 | 19 | 0.27 | 1.3 |
| Colvin Creek near Hoyt Lakes | 58 | 2015-2018 | 38 | 52 | 7 | 0.43 | 0.02 |
| Stoney Brook near Brookston | 192 | 2007-2018 | 23 | 63 | 10 | 0.32 | 0.31 |
| Partridge River at Hoyt Lakes | 270 | 1986-1988; 2002 | 37 | 52 | 5 | 0.40 | 0.03 |
| Partridge River near Hoyt Lakes | 333 | 2010-2018 | 37 | 48 | 7 | 0.40 | 0.21 |
| Swan River near Toivola | 620 | 2011-2018 | 32 | 43 | 7 | 0.26 | 1.2 |
| St Louis River near Aurora | 756 | 1986-1987; 2014-2015 | 32 | 53 | 8 | 0.36 | 0.27 |
| Whiteface River near Meadowlands | 1354 | 2012-2018 | 26 | 62 | 7 | 0.41 | 0.15 |
| St Louis River near Forbes | 1791 | 1986-1989; 2010-2018 | 34 | 49 | 7 | 0.38 | 0.49 |
| Cloquet River near Burnett | 2028 | 2009-2017 | 39 | 46 | 7 | 0.48 | 0.37 |
| St Louis River at Scanlon | 8884 | 1986-2018 | 30 | 53 | 7 | 0.35 | 0.45 |

*Table 2: Data used in the analysis of annual water yield and annual maximum peak daily streamflow.*

| Annual Water Yield | Basins Used | Equation 5 Key | Data Citation | Annual Maximum Daily Streamflow | Basins Used | Data Source |
|---|---|---|---|---|---|---|
| Annual precipitation* | K, STL | *P* | PRISM Climate Group, 2020 | Winter precipitation | K, STL | PRISM Climate Group, 2020 |
| Previous year's runoff ratio (to capture antecedent wetness) | K | | USGS, 2016; PRISM Climate Group, 2020 | Spring precipitation | K, STL | PRISM Climate Group, 2020 |
| September-October Precipitation (for antecedent wetness) | STL | | PRISM Climate Group, 2020 | September-October Precipitation (for antecedent wetness) | STL | PRISM Climate Group, 2020 |
| Annual average monthly temperature* | K, STL | | PRISM Climate Group, 2020 | Average monthly winter temperature | K, STL | PRISM Climate Group, 2020 |
| Annual average monthly dew point temperature* | K, STL | | PRISM Climate Group, 2020 | | | |
| Annual average minimum monthly vapor pressure deficit* | K, STL | | PRISM Climate Group, 2020 | | | |
| Annual average maximum monthly vapor pressure deficit* | K, STL | *VPD* | PRISM Climate Group, 2020 | | | |
| First principal component of: monthly maximum, minimum vapor pressure deficit, monthly mean air and dewpoint temperatures, and annual total Thornthwaite PET. Explained 62.6% of the total variance in those terms. | STL | *ET.PCA1* | PRISM Climate Group, 2020; SPEI Package in R | | | |
| Thornthwaite PET | K, STL | *PET* | PRISM Climate Group, 2020 SPEI package in R (Beguería & Vicente-Serrano, 2023) | | | |

*Table 3: Water yield on the Upper Kawishiwi catchment after the Pagami Creek Fire, N years after the fire. Years with > 90% confidence in water yield increases are marked with \*. Expected water yield was that based on the pre-fire model. Confidence that the water yield decreased equals one minus the confidence that water yield increased.*

| Years after the fire | 1 | 2 | 3 | 4 | 5 | 6 | 7 | 8 |
|---|---|---|---|---|---|---|---|---|
| Expected (sd) [mm] | 263 (58) | 274 (58) | 312 (59) | 175 (59) | 309 (64) | 346 (66) | 256 (56) | 295 (58) |
| Observed [mm] | 212 | 356 | 367 | 210 | 312 | 351 | 251 | 286 |
| Confidence that Water Yield Increased | 19% | 92% * | 83% | 73% | 52% | 54% | 46% | 44% |

*Table 4: ANCOVA-based annual maximum flows on the Upper Kawishiwi catchment after the Pagami Creek Fire. Expected peak flow was that based on the pre-fire model. Confidence that the peak flow decreased equals one minus the confidence that peak flow increased.*

| Years after the fire | 1 | 2 | 3 | 4 | 5 | 6 | 7 | 8 |
|---|---|---|---|---|---|---|---|---|
| Expected (sd) [mm/day] | 2.88 (1.16) | 3.27 (1.16) | 3.57 (1.19) | 2.36 (1.19) | 4.76 (1.39) | 3.87 (1.33) | 2.11 (1.17) | 3.69 (1.17) |
| Observed [mm/day] | 2.90 | 3.56 | 4.97 | 2.25 | 3.31 | 3.35 | 2.01 | 3.16 |
| Confidence that Peak Flow Increased | 51% | 60% | 88% | 47% | 14% | 35% | 46% | 32% |

*Table 5: Water Yield effect parameter for the St. Louis catchments LME-residuals model. Where our confidence that the water yield decreased is greater than 90%, we marked with * .*

| Catchment | Effect Parameter $b_r$ [mm of water yield change from expected, per additional percentage of forest disturbed in last 11 years or permanently converted] | $P(b_r < 0)$ [%] |
|---|---|---|
| Second Creek near Aurora | -19 [-25 to -12] | 100% * |
| Colvin Creek near Hoyt Lakes | 2 [-20 to 22] | 44% |
| Stoney Brook near Brookston | -4 [-31 to 22] | 59% |
| Partridge River at Hoyt Lakes | 3 [-6 to 12] | 28% |
| Partridge River near Hoyt Lakes | -2 [-13 to 10] | 59% |
| Swan River near Toivola | -9 [-34 to 17] | 73% |
| St Louis River near Aurora | 3 [-7 to 12] | 33% |
| Whiteface River near Meadowlands | 4 [-17 to 24] | 38% |
| St Louis River near Forbes | -13 [-18 to -8] | 100% * |
| Cloquet River near Burnett | 1 [-17 to 20] | 45% |
| St Louis River at Scanlon | -9 [-13 to -5] | 100% * |

*Table 6: Peak Flow effects for the St. Louis catchments LME-residuals model. Where confidence in peak flow decreases, or increases, were >90%, we marked with a * .*

| Catchment | Effect Parameter $b_r$ [m³/s / 100km² peak flow change from expected, per additional percentage of forest disturbed in last 11 years or permanently converted] | P($b_r$ < 0) [%] |
|---|---|---|
| Second Creek near Aurora | -0.3 [-0.7 to 0.05] | 92% * |
| Colvin Creek near Hoyt Lakes | 0.4 [-1.9 to 2.7] | 38% |
| Stoney Brook near Brookston | 3.3 [1.7 to 4.9] | <1% (>99% confidence $b_r$ > 0) * |
| Partridge River at Hoyt Lakes | 0.3 [-0.1 to 0.6] | 13% |
| Partridge River near Hoyt Lakes | -0.3 [-1.2 to 0.6] | 73% |
| Swan River near Toivola | -1.4 [-3.5 to 0.7] | 86% |
| St Louis River near Aurora | -0.4 [-0.7 to -0.08] | 98% * |
| Whiteface River near Meadowlands | 1.9 [1.0 to 2.8] | < 1% (>99% confidence $b_r$ > 0)* |
| St Louis River near Forbes | -0.2 [-0.4 to -0.01] | 96% * |
| Cloquet River near Burnett | 7.2 [2.0 to 12.2] | 1% (99% confidence $b_r$ > 0) * |
| St Louis River at Scanlon | -0.1 [-0.2 to 0.08] | 81% |

*Table 7: Forest disturbance and winter\*spring precipitation effects parameters, for the probabilistic model of Q2 streamflow on the St. Louis Basin. \* indicate high-confidence effects parameters where confidence in the effect being greater than or less than zero is >90%.*

| Catchment | Forest disturbance effect parameter [m³/s per additional percentage forest disturbance] | Precipitation effect parameter [m³/s per standard deviation of winter times spring precipitation] |
|---|---|---|
| Second Creek near Aurora | -0.13 (-0.33 to 0.08) | 0.19 (-0.25 to 0.67) |
| Colvin Creek near Hoyt Lakes | -0.37 (-1.1 to 0.38) | -0.01 (-4.1 to 4.6) |
| Stoney Brook near Brookston | 1.7 (-0.71 to 3.9) | 2.5 (1.2 to 3.8) * |
| Partridge River at Hoyt Lakes | -0.29 (-9.4 to 8.1) | 3.0 (-29 to 39) |
| Partridge River near Hoyt Lakes | -0.09 (-2.4 to 1.9) | 3.4 (1.4 to 5.5) * |
| Swan River near Toivola | -4.3 (-12 to 3.2) | 7.5 (0.56 to 14.4) * |
| St Louis River near Aurora | -1.5 (-5.4 to 1.8) | 2.6 (-6.0 to 12) |
| Whiteface River near Meadowlands | -0.91 (-17 to 14) | 11.1 (-22 to 47) |
| St Louis River near Forbes | -2.3 (-4.3 to -0.37) * | 13.3 (7.6 to 19) * |
| Cloquet River near Burnett | -10.7 (-27.7 to 5.8) | 23 (-31 to 80) |
| St Louis River at Scanlon | -9.0 (-21 to 3.0) | 92 (59 to 125) * |